

Light curve of pulses of gamma-ray bursts affected by the Doppler effect of fireballs

Yi-Ping Qin^{1,2}, Zhi-Bin Zhang^{1,3}, Fu-Wen Zhang² and Xiao-Hong Cui^{1,3}

¹National Astronomical Observatories/Yunnan Observatory, Chinese Academy of Sciences, P. O. Box 110, Kunming, Yunnan, 650011, P. R. China

²Physics Department, Guangxi University, Nanning, Guangxi, 530004, P. R. China

³ The Graduate School of the Chinese Academy of Sciences

Abstract

In this paper, we derive in a much detail the formula of count rates, in terms of the integral of time, of gamma-ray bursts based on the model of highly symmetric fireballs, where the Doppler effect of the expanding fireball surface is the key factor to be concerned. Different from previous studies, our analysis does not rely on any estimated methods, and the effect arising from the the limit of the time delay due to the curvature of the surface is carefully studied. Based on a quite robust theoretical ground, our analysis convinces the previous suggestion that the well known structure of FRED (a fast rise and an exponential decay) of pulses could be accounted for by the Doppler effect of the expanding fireball surface (called the curvature effect), where the exponential decay phase arises from the time delay of different parts of the surface and the rising portion is produced by the width of the local pulses. This character of FRED is independent of the Lorentz factor as long as the factor is large enough to represent a relativistic motion, and it is independent of the local structure of pulses. It is pointed out that, as can be deduced from previous studies where estimated methods were used or is analyzed in detail in this paper, due to the Doppler effect of the fireball surface, neglecting the area of $\theta > 1/\Gamma$ would lead a light curve, of a very narrow local pulse, with a cutoff tail in its decay phase, which we call a cutoff tail problem. If the local pulse concerned is short enough, this feature would become a criterion to pick out those sources with $\theta < 1/\Gamma$ from others. Local pulses suddenly deeming would produce light curves which are very sharp at their peaks, while exponential decay local pulses would lead to smooth light curves, which become observational features directly associated with the original character of pulses. In

addition we find that the impact of the rest frame radiation on the light curve of fireballs can be very obvious and should not be neglected.

keywords: **gamma-rays: bursts** — **gamma-rays: theory** — **relativity**

1 Introduction

Light curves of gamma-ray bursts (GRBs) vary enormously, suggesting that the temporal activity of the sources would be of a stochastic process (see, e.g., Fishman et al. 1994). However, some simple bursts with well-separated structure suggest that they may consist of fundamental units of emission such as pulses, and some pulses are seen to comprise a fast rise and an exponential decay (FRED), which can be well represented by an flexible empirical function (see, e.g., Norris et al. 1996).

Due to the observed great output rate of radiation, GRBs are assumed to undergo a stage of fireballs which expand relativistically (see, e.g., Goodman 1986; Paczynski 1986). As pointed out by Krolik & Pier (1991), relativistic bulk motion of the gamma-ray-emitting plasma can account for some phenomena of GRBs. For example, emission lines would be significantly broadened due to the curvature of the fireball surface where Doppler boosting factors varies from point to point (see, e.g., Mészáros & Rees 1998; Heiley et al. 1999; Qin 2003). Promisingly, the observed FRED structure was found to be interpreted by the curvature effect as the observed plasma moves relativistically towards us and appears to be locally isotropic (e.g., Fenimore et al. 1996, hereafter Paper I; Ryde & Petrosian 2002, hereafter Paper II; Kocevski et al. 2003). Light curves of pure fireballs can be approximately described in previous efforts where the delay of the observational time from the area concerned is estimated by assuming $\theta \sim 1/\Gamma$, where θ is the angle to the line of sight and Γ is Lorentz factor of the expansion.

As derived in detail in Paper II, a FRED pulse can be well described by the bolometric light curve of a shell shining continuously, which is

$$F(t) = F_0 \int_0^\infty \frac{f(t-x)}{(1+x/t_{ang})^2} dx, \quad (1)$$

where t_{ang} is the curvature timescale. For several reasons we want to modify this formula. First, we suspect that, due to the great output rate of the radiation observed, there might be some GRBs detected just undergoing the fireball stage, and therefore presenting a formula based on

the highly symmetric fireball model is necessary and it would be more suitable to describe light curves of these sources. Second, while other properties such as the whole output energy observed might be affected mildly, the decay tail of the light curve which was interpreted to be due to the curvature effect might obviously be affected by the conventional estimated method, since it is the curvature that makes the tail but the conventional estimating method ignores the detail of the curvature. Third, probably most importantly, we observe that the integral limit of equation (1) is not appropriately provided. Since the emission region (or, the radius of the fireball) is finite, the delay time [say, x in equation (1)] must also be limited. In fact, if the discussion is confined within $\theta \sim 1/\Gamma$, in consistent with the estimating method, the integral range would be $0 \leq x \leq t_{ang}$. With this integral range, we have Fig. 1, where the corresponding light curve is plotted. We find in this figure that, the limit of the integral range indeed affect the profile of the light curve significantly, both in the rising and decay phases of the curve. [Note that, if the whole fireball surface is concerned, equation (1) is also not applicable even when the integral limit will be derived from the whole surface, as equation (17) in Paper II will be no more valid for large values of θ .] It is noticed that, in Fig. 6 of Paper II (as well as Fig. 1 of this paper), the adopted duration of emission of the fireball shell is unlimited. Will this has any impacts on the light curve? This is also deserved an investigation.

In the following, we will first derive in a much detail the formula suitable for describing the light curve of highly symmetric fireballs (where, we will pay most of our attention to the integral limit which might be constrained by the concerned area of the fireball surface and/or the emission interval of time). Then we will apply the formula to the case of a local δ function pulse and will discuss in detail why the whole fireball surface instead of a fraction confined by $\theta \leq 1/\Gamma$ should be considered, and how a rest frame radiation form will affect the expected curve. Later we will study light curves of different forms of local pulses. A discussion will be presented in the last section.

2 General formula of count rates for highly symmetric fireballs

There are several papers published studying light curves of relativistically expanding fireballs (e.g., Paper I; Paper II). In the previous studies, a conventional estimated method (always referring to taking $\theta \leq 1/\Gamma$) is adopted, and the limit of the time delay due to the constraint of the finite

emission region is ignored. To find out if the effect arising from adopting the conventional method is significant, we present in the following a much detailed study on the same issue, where we will pay most of our attention to the integral limit which might be constrained by the concerned area of the fireball surface as well as the emission interval of time.

In the following we consider the case of a fireball expanding isotropically with a constant Lorentz factor.

For a radiation independent of direction, the expected flux of a fireball expanding with a constant Lorentz factor is (Qin 2002, hereafter Paper III)

$$f_\nu(t) = \frac{2\pi}{D^2} \int_{\tilde{\theta}_{\min}}^{\tilde{\theta}_{\max}} I_\nu(t_\theta, \nu) R^2(t_\theta) \cos \theta \sin \theta d\theta, \quad (2)$$

where ν is the observation frequency; t is the observation time; D is the distance of the fireball to the observer; θ is the angle, of the concerned differential surface ds_θ , of the fireball, to the line of sight; t_θ is the emission time (in the observer frame), called local time, of photons which emit from ds_θ ; $I_\nu(t_\theta, \nu)$ is the observer frame intensity; $R(t_\theta)$ is the radius of the fireball at time t_θ . The integral range of θ , $\tilde{\theta}_{\min}$ and $\tilde{\theta}_{\max}$, will be determined by the concerned area of the fireball surface as well as the emission ranges of the frequency and the local time. Applying the relation between the radius of the fireball and the observation time (see Paper III) we come to the following form of the flux:

$$f_\nu(t) = \frac{2\pi c^2 [(t - t_c - \frac{D}{c})\beta + \frac{R_c}{c}]^2}{D^2} \int_{\tilde{\theta}_{\min}}^{\tilde{\theta}_{\max}} \frac{I_\nu(t_\theta, \nu) \cos \theta \sin \theta}{(1 - \beta \cos \theta)^2} d\theta, \quad (3)$$

where t_c and R_c are constants.

We consider the situation that the area of the fireball surface concerned is confined within

$$\theta_{\min} \leq \theta \leq \theta_{\max} \quad (4)$$

and the emission time t_θ is confined within

$$t_c \leq t_{\theta,\min} \leq t_\theta \leq t_{\theta,\max}, \quad (5)$$

and besides them there are no other constraints to the integral limit of (2) or (3). According to (4) and (5), one can verify that the lower and upper integral limits of (3) could be determined by

$$\tilde{\theta}_{\min} = \cos^{-1} \min \left\{ \cos \theta_{\min}, \frac{t_{\theta,\max} - t + \frac{D}{c}}{(t_{\theta,\max} - t_c)\beta + \frac{R_c}{c}} \right\} \quad (6)$$

and

$$\tilde{\theta}_{\max} = \cos^{-1} \max \left\{ \cos \theta_{\max}, \frac{t_{\theta,\min} - t + \frac{D}{c}}{(t_{\theta,\min} - t_c)\beta + \frac{R_c}{c}} \right\}, \quad (7)$$

respectively (for a detailed derivation, one could refer to Paper III).

As shown by Paper III, t_θ and t are related by

$$t_\theta = \frac{t - t_c - \frac{D}{c} + \frac{R_c}{c} \cos \theta}{1 - \beta \cos \theta} + t_c. \quad (8)$$

From (8) one finds that, for any given values of t and θ , t_θ would be uniquely determined. If this value of t_θ is within the range of (5), then there will be photons emitted at t_θ from the small surface area of θ reaching the observer at t [when θ is within the range of (4), this small area would be included in the above integral, otherwise it would not]. Obviously, for a certain value of θ , the range of t depends on the range of t_θ . Inserting (8) into (5) and applying (4) we obtain

$$(1 - \beta \cos \theta_{\min}) t_{\theta, \min} + (t_c \beta - \frac{R_c}{c}) \cos \theta_{\min} + \frac{D}{c} \leq t \leq (1 - \beta \cos \theta_{\max}) t_{\theta, \max} + (t_c \beta - \frac{R_c}{c}) \cos \theta_{\max} + \frac{D}{c}. \quad (9)$$

It suggests clearly that observation time t is limited when emission time t_θ is limited.

If during some period the radiation of the fireball is dominated by a certain mechanism, then within this interval of time the intensity can be expressed as:

$$I_\nu(t_\theta, \nu) = I(t_\theta) g_\nu(\nu) = I(t_\theta) \frac{g_{0, \nu}(\nu_{0, \theta})}{(1 - \beta \cos \theta)^3 \Gamma^3}, \quad (10)$$

where $\nu_{0, \theta}$ is the rest frame emission frequency corresponding to ν (they are related by the Doppler effect), $I(t_\theta)$ represents the development of the intensity magnitude in the observer frame, and $g_\nu(\nu)$ and $g_{0, \nu}(\nu_{0, \theta})$ describe the observer frame and the rest frame radiation mechanisms, respectively. In deriving the last equivalency, the Lorentz invariance of $g_\nu(\nu)/\nu^3$ and the Doppler effect are applied. Flux (3) then can be written as

$$f_\nu(t) = \frac{2\pi c^2 [(t - t_c - \frac{D}{c})\beta + \frac{R_c}{c}]^2}{D^2 \Gamma^3} \int_{\tilde{\theta}_{\min}}^{\tilde{\theta}_{\max}} \frac{I(t_\theta) g_{0, \nu}(\nu_{0, \theta}) \cos \theta \sin \theta}{(1 - \beta \cos \theta)^5} d\theta, \quad (11)$$

where $\tilde{\theta}_{\min}$ and $\tilde{\theta}_{\max}$ are determined by (6) and (7), respectively, $\nu_{0, \theta}$ and ν are related by the Doppler effect, and t is confined by (9).

Light curves of gamma-ray bursts are always presented in terms of count rates within an energy range. The count rate within energy channel $[\nu_1, \nu_2]$ is determined by

$$\frac{dn(t)}{dt} = \int_{\nu_1}^{\nu_2} \frac{f_\nu(t)}{h\nu} d\nu. \quad (12)$$

Applying (11) leads to

$$\frac{dn(t)}{dt} = \frac{2\pi c^2 [(t - t_c - \frac{D}{c})\beta + \frac{R_c}{c}]^2 \int_{\tilde{\theta}_{\min}}^{\tilde{\theta}_{\max}} \frac{I(t_\theta) \cos \theta \sin \theta}{(1 - \beta \cos \theta)^5} d\theta \int_{\nu_1}^{\nu_2} \frac{g_{0, \nu}(\nu_{0, \theta})}{\nu} d\nu}{h D^2 \Gamma^3}. \quad (13)$$

Assign

$$\tau_\theta \equiv \frac{t_\theta - t_c}{\frac{R_c}{c}}, \quad (14)$$

$$\tau_{\theta,\min} \equiv \frac{t_{\theta,\min} - t_c}{\frac{R_c}{c}}, \quad (15)$$

$$\tau_{\theta,\max} \equiv \frac{t_{\theta,\max} - t_c}{\frac{R_c}{c}}, \quad (16)$$

and

$$\tau \equiv \frac{t - t_c - \frac{D}{c} + \frac{R_c}{c}}{\frac{R_c}{c}}. \quad (17)$$

One would find

$$\tau_\theta = \frac{\tau - (1 - \cos \theta)}{1 - \beta \cos \theta}, \quad (18)$$

$$\tau_{\theta,\min} \leq \tau_\theta \leq \tau_{\theta,\max}, \quad (19)$$

and

$$1 - \cos \theta_{\min} + (1 - \beta \cos \theta_{\min})\tau_{\theta,\min} \leq \tau \leq 1 - \cos \theta_{\max} + (1 - \beta \cos \theta_{\max})\tau_{\theta,\max} \quad (20)$$

[which is the range of τ within which the radiation within (4) and (5) is observable].

One could verify that, in terms of the integral of τ_θ , count rate (13) becomes

$$C(\tau) = \frac{2\pi R_c^3 \int_{\tau_{\theta,\min}}^{\tau_{\theta,\max}} \tilde{I}(\tau_\theta) (1 + \beta \tau_\theta)^2 (1 - \tau + \tau_\theta) d\tau_\theta \int_{\nu_1}^{\nu_2} \frac{g_{0,\nu}(\nu_{0,\theta})}{\nu} d\nu}{hc D^2 \Gamma^3 (1 - \beta)^2 (1 + k\tau)^2}, \quad (21)$$

where τ is confined by (20),

$$C(\tau) \equiv \frac{dn[t(\tau)]}{d\tau}, \quad (22)$$

$$\tilde{I}(\tau_\theta) \equiv I[t_\theta(\tau_\theta)], \quad (23)$$

$$k \equiv \frac{\beta}{1 - \beta}, \quad (24)$$

and $\nu_{0,\theta}$ and ν are related by

$$\nu_{0,\theta} = \frac{(1 + k\tau)(1 - \beta)\Gamma}{1 + \beta\tau_\theta} \nu, \quad (25)$$

while $\tilde{\tau}_{\theta,\min}$ and $\tilde{\tau}_{\theta,\max}$ are determined by

$$\tilde{\tau}_{\theta,\min} = \max\{\tau_{\theta,\min}, \frac{\tau - 1 + \cos \theta_{\max}}{1 - \beta \cos \theta_{\max}}\} \quad (26)$$

and

$$\tilde{\tau}_{\theta,\max} = \min\{\tau_{\theta,\max}, \frac{\tau - 1 + \cos \theta_{\min}}{1 - \beta \cos \theta_{\min}}\}, \quad (27)$$

respectively.

3 Count rate of local δ function pulses

Previous studies on the light curve of a local δ function pulse can be found in Paper I and Paper II, where, as mentioned above, the limit of the time delay due to the constraint of the finite emission region is ignored. Here, we study the same light curve by applying the formula of count rates derived above, in which, the mentioned constraint is taken into account and, in addition, other factors possibly ignored by previous studies would be maintained.

Let

$$I(t_\theta) = I_0 \delta(t_\theta - t_{\theta,0}) \quad (t_{\theta,\min} \leq t_\theta \leq t_{\theta,\max}), \quad (28)$$

with

$$t_{\theta,\min} < t_{\theta,0} < t_{\theta,\max}, \quad (29)$$

where I_0 is a constant. In terms of τ_θ , we would get

$$\tilde{I}(\tau_\theta) = \frac{cI_0}{R_c} \delta(\tau_\theta - \tau_{\theta,0}) \quad (\tau_{\theta,\min} \leq \tau_\theta \leq \tau_{\theta,\max}) \quad (30)$$

and

$$\tau_{\theta,\min} < \tau_{\theta,0} < \tau_{\theta,\max}, \quad (31)$$

where

$$\tau_{\theta,0} \equiv \frac{t_{\theta,0} - t_c}{\frac{R_c}{c}}. \quad (32)$$

One can check that, when

$$1 - \cos \theta_{\min} + (1 - \beta \cos \theta_{\min}) \tau_{\theta,0} < \tau < 1 - \cos \theta_{\max} + (1 - \beta \cos \theta_{\max}) \tau_{\theta,0} \quad (33)$$

(which is the range of τ within which the radiation of the local δ function pulse over the concerned area is observable), the following would be satisfied:

$$\tilde{\tau}_{\theta,\min} < \tau_{\theta,0} < \tilde{\tau}_{\theta,\max}. \quad (34)$$

Inserting (30) into (21) and applying (34) one would get

$$C(\tau) = \frac{2\pi R_c^2 I_0 \int_{\nu_1}^{\nu_2} \frac{g_{0,\nu}(\nu_{0,\theta})}{\nu} d\nu}{h D^2} C_0(\tau), \quad (35)$$

where τ is confined by (33),

$$C_0(\tau) \equiv \frac{(1 + \beta \tau_{\theta,0})^2 (1 + \tau_{\theta,0} - \tau)}{\Gamma^3 (1 - \beta)^2 (1 + k\tau)^2} \quad (36)$$

and

$$\nu_{0,\theta} = \frac{(1+k\tau)(1-\beta)\Gamma}{1+\beta\tau_{\theta,0}}\nu. \quad (37)$$

It shows that, due to the Doppler effect (or the curvature effect) referring to the concerned area of the fireball surface, a local δ function pulse would produce an observed pulse bearing the shape of $C_0(\tau)$, where τ is confined by (33), modified by the rest frame spectrum of the fireball.

First, let us consider the whole fireball surface. In this case we take

$$\theta_{\min} = 0 \quad \text{and} \quad \theta_{\max} = \frac{\pi}{2}, \quad (38)$$

and get from (33) that

$$(1-\beta)\tau_{\theta,0} < \tau < 1 + \tau_{\theta,0}. \quad (39)$$

Adopting $\tau_{\theta,0} = 0$, we get $0 < \tau < 1$. Presented in Figs. 2 and 3 we make the curve of $C_0(\tau)$ by adopting $\Gamma = 10$ and $\Gamma = 100$, respectively. The figures show that, function $C_0(\tau)$ confined by (39) bears a feature of an exponential decay, and the profile remains almost the same for different values of the Lorentz factor. It is interesting that the upper limit of τ [see (39)] does not prevent the formation of the exponential decay tail.

One can verify that, the maximum value of $C_0(\tau)$ is

$$C_{0,p} = \frac{1}{\Gamma(\Gamma - \sqrt{\Gamma^2 - 1})^2} \frac{R(t_{\theta,0})}{R_c}, \quad (40)$$

while the width of $C_0(\tau)$ can be determined by

$$\Delta\tau_{FWHM} = \frac{(\Gamma - \sqrt{\Gamma^2 - 1})(\sqrt{2\Gamma^2 - 1} - \Gamma)}{\Gamma^2 - 1} \frac{R(t_{\theta,0})}{R_c}, \quad (41)$$

and the relation between them is

$$C_{0,p} = \frac{\Gamma^2 - 1}{\Gamma(\Gamma - \sqrt{\Gamma^2 - 1})^3(\sqrt{2\Gamma^2 - 1} - \Gamma)} \Delta\tau_{FWHM}. \quad (42)$$

(For a detailed derivation one could refer to Appendix A).

Ignoring the effect of the rest frame radiation form (which will be discussed below), $C_{0,p}$ and $\Delta\tau_{FWHM}$ will serve as the observed peak and width of the light curve of the local δ function pulse.

When $\Gamma \gg 1$, one can come to

$$C_{0,p} \simeq 4\Gamma \frac{R(t_{\theta,0})}{R_c} \quad (\Gamma \gg 1), \quad (43)$$

$$\Delta\tau_{FWHM} \simeq \frac{\sqrt{2} - 1}{2\Gamma^2} \frac{R(t_{\theta,0})}{R_c} \quad (\Gamma \gg 1), \quad (44)$$

and

$$C_{0,p} \simeq \frac{8\Gamma^3}{\sqrt{2}-1} \Delta\tau_{FWHM} \quad (\Gamma \gg 1). \quad (45)$$

It shows, both the observed peak and width of the count rate of the local δ function pulse are proportional to the size of the fireball. While the former rises linearly with respect to the increase of the Lorentz factor, the latter, as generally known, decays rapidly following the law of Γ^{-2} (see, e.g. Fenimore et al. 1993), which naturally explains why for many bursts very short time scales, as small as a few *ms*, of pulses have been observed. For a certain value of the Lorentz factor, quantities $C_{0,p}$ and $\Delta\tau_{FWHM}$ are proportional to each other.

Combining (43) and (44) one gets

$$C_{0,p}^2 \Delta\tau_{FWHM} \simeq 8(\sqrt{2}-1) \left(\frac{R(t_{\theta,0})}{R_c} \right)^3 \quad (\Gamma \gg 1). \quad (46)$$

This suggests that, for a same kind of fireball sources, if their difference is merely due to the Lorentz factor, the product of the square of the peak count rate and the width of the light curve of their very narrow local pulses would be the same. This provides a statistical approach to test the fireball model with pulses of GRBs. For a source, if the intensity of its pulses remains unchanged, one can expect a high pulse coupling with a small width while a low pulse coupling with a larger one.

Let $\Delta\tau$ be the interval of the observable time of the local δ function pulse. It would be determined by (39). According to (A6.) and (A8.) we get

$$\frac{R(t_{\theta,0})}{R_c} = \Delta\tau. \quad (47)$$

Then (44) becomes

$$\Delta\tau_{FWHM} \simeq \frac{\sqrt{2}-1}{2\Gamma^2} \Delta\tau \quad (\Gamma \gg 1). \quad (48)$$

With this one finds that the observed width of the light curve of the local δ function pulse would be several orders of magnitude smaller than the limit of the observable time when the Lorentz factor is large enough. This explains why the upper limit of τ does not prevent the formation of the exponential decay tail shown in Figs. 2 and 3. However, when the area concerned is quite small, the situation might be much different.

Let us turn to study the effect of the limit of the time delay, which refers to the small area with $\theta \leq 1/\Gamma$. Taking

$$\theta_{\min} = 0 \quad \text{and} \quad \theta_{\max} = \frac{1}{\Gamma}, \quad (49)$$

we get from (33) that

$$(1 - \beta)\tau_{\theta,0} < \tau < 1 - \cos \frac{1}{\Gamma} + (1 - \beta \cos \frac{1}{\Gamma})\tau_{\theta,0}, \quad (50)$$

when Γ is large enough which leads to

$$(1 - \beta)\tau_{\theta,0} < \tau < \frac{1 + 2\tau_{\theta,0}}{2\Gamma^2} \quad (\Gamma \gg 1). \quad (51)$$

Adopting $\tau_{\theta,0} = 0$, we get $0 < \tau < 1/2\Gamma^2$. The curves of $C_0(\tau) - \tau$ for $\Gamma = 10$ and 100 in this case are also presented in Figs. 2 and 3, respectively. It shows that, due to the Doppler effect of the fireball surface, neglecting the area of $\theta > 1/\Gamma$ would lead a light curve, of a local δ function pulse, with a cutoff tail in its decay phase, which we call a cutoff tail problem, suggesting that if only the area of $\theta < 1/\Gamma$ is considered, the decay phase of the corresponding light curve would not be a full exponentially decaying one (the case of a longer local pulse will be discussed in late sections). [A similar result can be deduced from the dotted lines presented in Fig. 4 of Paper I, where an approximate form of the formula was used.] As shown in Appendix A, the count rate at $\theta = 1/\Gamma$ is only a quarter of the peak. The missed part of the light curve is obviously observable. But as shown in Fig. 1, why the tail of the light curve presented in Paper II does not exhibit such a cutoff feature even when a limited time delay is considered? The answer is that the emission time concerned there is unlimited. In fact, as shown in Paper II, Fig. 6 there (and Fig. 1 here) does not represent the case of a local δ function pulse. When the emission time is limited and the interval is short enough, a similar result would be seen (see Fig. 4 for an illustration, where a finite emission time interval, $0 \leq t \leq t_{dyn}$, is assumed).

Compared with that presented in Paper I and Paper II, one finds from (36) that the factor of $(1 + \tau_{\theta,0} - \tau)$ was previously ignored. When $\tau \ll 1 + \tau_{\theta,0}$, this factor is negligible, while when τ is comparable to $1 + \tau_{\theta,0}$, this factor would play a role. However, as shown in Figs. 2 and 3, a large value of the Lorentz factor will make the decay phase of the light curve very short, so that the interesting value of τ will be very small and then the factor of $(1 + \tau_{\theta,0} - \tau)$ would not be important.

Another factor affecting the light curve is the integral of the rest frame radiation. When adopting $g_{0,\nu}(\nu_{0,\theta}) = \nu_{0,\theta}^{-\alpha_f}$, one obtains $\int_{\nu_1}^{\nu_2} [g_{0,\nu}(\nu_{0,\theta})/\nu] d\nu = g_0(1 + k\tau)^{-\alpha_f}$, where g_0 is a constant. A product of this term with the term of $(1 + k\tau)^{-2}$ in $C_0(\tau)$ is similar to that obtained in Paper I. However, observation suggests that the common radiation form of GRBs is the so-called Band

function (Band et al. 1993) which was frequently, and rather successfully, employed to fit the spectra of the sources (see, e.g., Schaefer et al. 1994; Ford et al. 1995; Preece et al. 1998, 2000). Paper III shows that the observed radiation form would only be affected slightly by the fireball Doppler effect. Therefore it is expected that many fireball sources might take a rest frame radiation form of the Band function, rather than a power law one (as adopted in Paper I). In this way, the effect of the radiation mechanism on the light curve might be much different.

Following is the empirical radiation form of GRBs proposed by Band et al. (1993), the so-called Band function:

$$g_{0,\nu,B}(\nu_{0,\theta}) = \begin{cases} \left(\frac{\nu_{0,\theta}}{\nu_{0,p}}\right)^{1+\alpha_0} \exp[-(2+\alpha_0)\frac{\nu_{0,\theta}}{\nu_{0,p}}] & \left(\frac{\nu_{0,\theta}}{\nu_{0,p}} < \frac{\alpha_0-\beta_0}{2+\alpha_0}\right) \\ \left(\frac{\alpha_0-\beta_0}{2+\alpha_0}\right)^{\alpha_0-\beta_0} \exp(\beta_0-\alpha_0)\left(\frac{\nu_{0,\theta}}{\nu_{0,p}}\right)^{1+\beta_0} & \left(\frac{\nu_{0,\theta}}{\nu_{0,p}} \geq \frac{\alpha_0-\beta_0}{2+\alpha_0}\right) \end{cases}, \quad (52)$$

where subscript B represents the word Band, p stands for peak, α_0 and β_0 are the lower and higher indexes, respectively. Typical values coming from statistical analysis, of the lower and higher indexes of the Band function, are $\alpha_0 = -1$ and $\beta_0 = -2.25$ (Preece et al. 1998, 2000), respectively. As mentioned above, the shape of rest frame spectra is not significantly changed by the expansion of the fireball. We take $g_{0,\nu}(\nu_{0,\theta}) = g_{0,\nu,B}(\nu_{0,\theta})$ and adopt $\alpha_0 = -1$ and $\beta_0 = -2.25$ to study the effect of the rest frame spectrum on the light curve of a local δ function pulse. Shown in Figs. 5 and 6 are the light curves of $C(\tau)$ determined by (35), calculated within the frequency range of $50 \leq \nu/\nu_{0,p} \leq 100$, for $\Gamma = 10$ and 100 , respectively, where $C(\tau)$ is normalized to the peak of the corresponding $C_0(\tau)$. We find from these figures that the impact of the rest frame radiation on the light curve can be very obvious.

4 Count rate of local pulses with a certain value of width

In this section, we study the light curve of local pulses with a certain value of width. A typical and very simple one is a local rectangle pulse, which will be studied in a much detail. Other forms of local pulses will also be studied and be compared with the rectangle one. The limit of the time delay due to the constraint of the finite emission region will be taken into account and other factors possibly affecting the light curve will also be investigated.

4.1 The case of local rectangle pulses

To consider a local rectangle pulse we assume

$$I(t_\theta) = \begin{cases} I_0 & (t_\theta < t_{\theta,\min} \quad \text{and} \quad t_{\theta,\max} < t_\theta) \\ 0 & (t_{\theta,\min} \leq t_\theta \leq t_{\theta,\max}) \end{cases}, \quad (53)$$

where I_0 is a constant. From (53) we can come to

$$\tilde{I}(\tau_\theta) = \begin{cases} I_0 & (\tau_{\theta,\min} \leq \tau_\theta \leq \tau_{\theta,\max}) \\ 0 & \text{and} \\ & \tau_{\theta,\max} < \tau_\theta \end{cases}, \quad (54)$$

where, (14), (15), (16) and (23) are applied.

One finds from (26) and (27) that

$$\tau_{\theta,\min} \leq \tilde{\tau}_{\theta,\min} \quad (55)$$

and

$$\tilde{\tau}_{\theta,\max} \leq \tau_{\theta,\max}. \quad (56)$$

Inserting (54) into (21) yields

$$C(\tau) = \frac{2\pi R_c^3 I_0 \int_{\tau_{\theta,\min}}^{\tilde{\tau}_{\theta,\max}} (1 + \beta\tau_\theta)^2 (1 - \tau + \tau_\theta) d\tau_\theta \int_{\nu_1}^{\nu_2} \frac{g_{0,\nu}(\nu_{0,\theta})}{\nu} d\nu}{hcD^2 \Gamma^3 (1 - \beta)^2 (1 + k\tau)^2}, \quad (57)$$

where, (55) and (56) are applied. This is the formula with which the count rate of a local rectangle pulse can be calculated.

To focus on how the local width of pulses affects the observed profile, here we ignore the possible effect from the spectrum and assume a δ function one:

$$g_{0,\nu}(\nu_{0,\theta}) = \delta(\nu_{0,\theta} - \nu_{0,0}) \quad (\nu_{0,\min} \leq \nu_{0,\theta} \leq \nu_{0,\max}), \quad (58)$$

with

$$\nu_{0,\min} < \nu_{0,0} < \nu_{0,\max}. \quad (59)$$

In the following, we assume $\beta > 0$. Applying (25), we can rewrite (58) as

$$\tilde{g}_{0,\nu}(\nu, \tau_\theta, \tau) = \delta\left[\frac{(1 + k\tau)(1 - \beta)\Gamma}{1 + \beta\tau_\theta}(\nu - \nu_0)\right] \quad (\nu_{\min} \leq \nu \leq \nu_{\max}), \quad (60)$$

where

$$\tilde{g}_{0,\nu}(\nu, \tau_\theta, \tau) \equiv g_{0,\nu}[\nu_{0,\theta}(\nu, \tau_\theta, \tau)], \quad (61)$$

$$\nu_0 \equiv \frac{1 + \beta\tau_\theta}{\Gamma(1 - \beta)(1 + k\tau)} \nu_{0,0}, \quad (62)$$

$$\nu_{\min} \equiv \frac{1 + \beta\tau_\theta}{\Gamma(1 - \beta)(1 + k\tau)} \nu_{0,\min} \quad (63)$$

and

$$\nu_{\max} \equiv \frac{1 + \beta\tau_\theta}{\Gamma(1 - \beta)(1 + k\tau)} \nu_{0,\max}. \quad (64)$$

From (59) we find

$$\nu_{\min} < \nu_0 < \nu_{\max}, \quad (65)$$

where, (62), (63) and (64) are applied. According to the property of the δ function, we can rewrite (60) as

$$\tilde{g}_{0,\nu}(\nu, \tau_\theta, \tau) = \frac{1 + \beta\tau_\theta}{(1 + k\tau)(1 - \beta)\Gamma} \delta(\nu - \nu_0) \quad (\nu_{\min} \leq \nu \leq \nu_{\max}), \quad (66)$$

Suppose

$$\nu_1 < \nu_{\min} \quad (67)$$

and

$$\nu_{\max} < \nu_2. \quad (68)$$

Therefore,

$$\nu_1 < \nu_0 < \nu_2. \quad (69)$$

Replacing $g_{0,\nu}(\nu_0, \theta)$ in (57) with $\tilde{g}_{0,\nu}(\nu, \tau_\theta, \tau)$ shown by (66) we obtain

$$C(\tau) = \frac{2\pi R_c^3 I_0}{\nu_0 h c D^2 \Gamma^4 (1 - \beta)^3} \frac{\int_{\tilde{\tau}_{\theta,\min}}^{\tilde{\tau}_{\theta,\max}} (1 + \beta\tau_\theta)^3 (1 - \tau + \tau_\theta) d\tau_\theta}{(1 + k\tau)^3}, \quad (70)$$

Integrating (70) yields

$$C(\tau) = \frac{2\pi R_c^3 I_0}{5\nu_0 h c D^2 \Gamma^4 \beta^2 (1 - \beta)^3} \{ [(1 + \beta\tilde{\tau}_{\theta,\max})^5 - (1 + \beta\tilde{\tau}_{\theta,\min})^5] (1 + k\tau)^{-3} - \frac{5}{4}(1 - \beta)[(1 + \beta\tilde{\tau}_{\theta,\max})^4 - (1 + \beta\tilde{\tau}_{\theta,\min})^4] (1 + k\tau)^{-2} \}, \quad (71)$$

where $\tilde{\tau}_{\theta,\min}$ and $\tilde{\tau}_{\theta,\max}$ are determined by (26) and (27), respectively. This is the formula for calculating the count rate of the local rectangle pulse which ignores the effect of spectra.

To make the plot of $C(\tau)$, we consider the cases of the whole fireball surface and the small area of $\theta \leq 1/\Gamma$. In the first case, (38) is applicable, and then from (26), (27) and (20) we get

$$\tilde{\tau}_{\theta,\min} = \max\{\tau_{\theta,\min}, \tau - 1\}, \quad (72)$$

$$\tilde{\tau}_{\theta,\max} = \min\{\tau_{\theta,\max}, \frac{\tau}{1 - \beta}\}, \quad (73)$$

and

$$(1 - \beta)\tau_{\theta,\min} \leq \tau \leq 1 + \tau_{\theta,\max}, \quad (74)$$

respectively. In the second case, (49) is applicable, and then we obtain

$$\tilde{\tau}_{\theta,\min} = \max\{\tau_{\theta,\min}, \frac{\tau - 1 + \cos \frac{1}{\Gamma}}{1 - \beta \cos \frac{1}{\Gamma}}\}, \quad (75)$$

$$\tilde{\tau}_{\theta,\max} = \min\{\tau_{\theta,\max}, \frac{\tau}{1-\beta}\}, \quad (76)$$

and

$$(1-\beta)\tau_{\theta,\min} \leq \tau \leq 1 - \cos \frac{1}{\Gamma} + (1-\beta \cos \frac{1}{\Gamma})\tau_{\theta,\max}. \quad (77)$$

Profiles of $C(\tau)$ determined by (71) for the two cases are presented in Figs. 7 and 8, where we take $\pi R_c^3 I_0 / \nu_0 h c D^2 = 1$, $\Gamma = 10$ and $\tau_{\theta,\min} = 0$. Figs. 7 and 8 are made by adopting $\tau_{\theta,\max} = 0.2$ and $\tau_{\theta,\max} = 2$, respectively. The two figures show explicitly a structure of FRED, suggesting that, such pulses can arise from a fireball surface when the local pulse involved lasts an interval of time (in contrast with it, there exists only an exponential decay phase in the light curve of a local δ function pulse, for which no rising phase can be seen). We learn from this that the exponential decay phase is due to the curvature effect and the rising portion of FRED pulses is produced by the width of the local pulse. As is known, it is the width of the local pulse that leads to the rising phase (see, e.g., Paper I) (for a more detailed analysis of the rising phase one could refer to Appendix B). One finds that the less the width of the local pulse, the narrower the observed rising phase. We suspect that, for many GRBs, FRED pulses observed might merely be due to the expanding motion of fireballs. When taking different values of Γ , we find almost the same form of curves, suggesting that the character of FRED is a consequence of the expanding motion of fireballs as long as the motion is relativistic, no matter how large the Lorentz factor is. The cutoff tail feature is also observed in the two figures, with the longer the local pulse the less obvious the feature.

To study the impact of the rest frame radiation form on the light curve of local rectangle pulses, we employ the same Band function form of radiation, where $\alpha_0 = -1$ and $\beta_0 = -2.25$ are adopted. The count rate is determined by (57), where $g_{0,\nu}(\nu_{0,\theta})$ would be replaced by $g_{0,\nu,B}(\nu_{0,\theta})$ shown in (52) and $\nu_{0,\theta}$ is related with ν by (25). Once more we will consider the two cases of the whole fireball surface and the small area of $\theta \leq 1/\Gamma$. As shown above, for the whole fireball surface, $\tilde{\tau}_{\theta,\min}$ and $\tilde{\tau}_{\theta,\max}$ would be determined by (72) and (73), respectively, while τ would be confined by (74). For the small area of $\theta \leq 1/\Gamma$, $\tilde{\tau}_{\theta,\min}$ and $\tilde{\tau}_{\theta,\max}$ would be determined by (75) and (76), respectively, while τ would be confined by (77).

Profiles of $C(\tau)$ determined by (57), calculated within the frequency range of $50 \leq \nu / \nu_{0,p} \leq 100$, for the two cases are presented in Figs. 9 and 10, where we take $\Gamma = 10$ and $\tau_{\theta,\min} = 0$. Figs. 9 and 10 are made by adopting $\tau_{\theta,\max} = 0.2$ and $\tau_{\theta,\max} = 2$, respectively. For the sake of comparison, light curves in Figs. 7 and 8 for the case of the whole fireball surface are also plotted. Thus, $C(\tau)$

is normalized to the peak of the corresponding curve of Fig. 7 or 8.

The two figures also show explicitly a structure of FRED. The profiles of the curves are also affected by the rest frame radiation form. Compared with Fig. 5 we find that, due to the width of the local pulse, the impact of the rest frame radiation form on the profile of the light curves is much less obvious (the curves in Fig. 5 are those arise from a local δ function pulse which represents a pulse with no width).

4.2 The case of other forms of local pulses

Here we study if different forms of local pulses would lead to much different forms of expected light curves. In the following we consider several forms of local pulses other than the rectangle one.

a) Local pulse with a linear rise and a linear decay

The intensity is assumed to be

$$\tilde{I}(\tau_\theta) = I_0 \left\{ \begin{array}{ll} \frac{\tau_\theta - \tau_{\theta,\min}}{\tau_{\theta,\max}/2 - \tau_{\theta,\min}} & (\tau_{\theta,\min} \leq \tau_\theta \leq \tau_{\theta,\max}/2) \\ 1 - \frac{\tau_\theta - \tau_{\theta,\max}/2}{\tau_{\theta,\max} - \tau_{\theta,\max}/2} & (\tau_{\theta,\max}/2 < \tau_\theta \leq \tau_{\theta,\max}) \end{array} \right. . \quad (78)$$

We employ the same Band function radiation form with $\alpha_0 = -1$ and $\beta_0 = -2.25$ to make the light curve. The count rate is determined by (21), where $g_{0,\nu}(\nu_{0,\theta})$ would be replaced by $g_{0,\nu,B}(\nu_{0,\theta})$ shown in (52), and $\nu_{0,\theta}$ is related with ν by (25). We also consider the two cases of the whole fireball surface and the small area of $\theta \leq 1/\Gamma$. For the whole fireball surface, $\tilde{\tau}_{\theta,\min}$ and $\tilde{\tau}_{\theta,\max}$ would be determined by (72) and (73), respectively, while τ would be confined by (74). For the small area of $\theta \leq 1/\Gamma$, $\tilde{\tau}_{\theta,\min}$ and $\tilde{\tau}_{\theta,\max}$ would be determined by (75) and (76), respectively, while τ would be confined by (77).

Profiles of $C(\tau)$ determined by (21), of this intensity, calculated within the frequency range of $50 \leq \nu/\nu_{0,p} \leq 100$, for the two cases are presented in Figs. 11 and 12, where we take $\Gamma = 10$, $\tau_{\theta,\min} = 0$, and $2\pi R_c^3 I_0 / hcD^2 = 1$. Figs. 11 and 12 are made by adopting $\tau_{\theta,\max} = 0.2$ and $\tau_{\theta,\max} = 2$, respectively. For the sake of comparison, light curves in Figs. 9 and 10 for the case of the whole fireball surface are also plotted, where they are normalized to the peak of the corresponding curves analyzed here, and their variable, τ , is re-scaled so that the peak count rate as well as the FWHM of the decay portion locate at the same positions of those of the corresponding curves analyzed here. The two figures also show a structure of FRED, suggesting that the character of FRED is independent of the local structure of pulses. It is indeed a consequence of the expanding motion of fireballs. Different from those in Figs. 9 and 10, the curves of Figs. 11 and 12 are less

sharp around the position of the peak count rate. A bend in the rising portion of the curves is visible, and the longer the local pulse the more obvious the bend. The two figures also reveal that the larger the width of the local pulse the less sharp of the light curve at the peak and the position where the cutoff tail appears. From Fig. 12 we find it interesting that, if local pulses last a sufficient interval of time, the profile of the one deeming gradually would be more concentrated (see the solid line) than that of the one deeming suddenly (see the dot line).

b) Local pulse with a linear rise

The intensity is assumed to be

$$\tilde{I}(\tau_\theta) = I_0 \frac{\tau_\theta - \tau_{\theta,\min}}{\tau_{\theta,\max} - \tau_{\theta,\min}} \quad (\tau_{\theta,\min} \leq \tau_\theta \leq \tau_{\theta,\max}). \quad (79)$$

Profiles of $C(\tau)$ determined by (21), of this intensity, are presented in Figs. 13 and 14, where we take the same parameters adopted in Figs. 11 and 12.

c) Local pulse with a linear decay

The intensity is assumed to be

$$\tilde{I}(\tau_\theta) = I_0 \left(1 - \frac{\tau_\theta - \tau_{\theta,\min}}{\tau_{\theta,\max} - \tau_{\theta,\min}}\right) \quad (\tau_{\theta,\min} < \tau_\theta \leq \tau_{\theta,\max}). \quad (80)$$

Profiles of $C(\tau)$ determined by (21), of this intensity, are presented in Figs. 15 and 16, where we take the same parameters adopted in Figs. 11 and 12.

d) Local pulse with an exponential rise and an exponential decay

The intensity is assumed to be

$$\tilde{I}(\tau_\theta) = I_0 \left\{ \begin{array}{ll} \exp(\tau_\theta/\sigma) & (\tau_{\theta,\min} \leq \tau_\theta < 0) \\ \exp(-\tau_\theta/\sigma) & (0 \leq \tau_\theta) \end{array} \right. . \quad (81)$$

Note that, since $1 + \beta\tau_\theta = R(t_\theta)/R_c > 0$ (see Appendix A), $\tau_\theta > -1/\beta$. That provides a constraint to the lower limit of τ_θ , i. e., $\tau_{\theta,\min} > -1/\beta$. Here we take $\tau_{\theta,\min} = -1$, and adopt $\sigma = 0.2$ and $\sigma = 2$ to make Figs. 17 and 18, respectively. Other parameters are the same of those adopted in Figs. 11 and 12.

e) Local pulse with an exponential rise

The intensity is assumed to be

$$\tilde{I}(\tau_\theta) = I_0 \exp(\tau_\theta/\sigma) \quad (\tau_{\theta,\min} \leq \tau_\theta \leq \tau_{\theta,\max}). \quad (82)$$

Here we take $\tau_{\theta,\max} = 0$ to make Figs. 19 and 20. Other parameters are the same as those adopted in Figs. 17 and 18.

f) Local pulse with an exponential decay

The intensity is assumed to be

$$\tilde{I}(\tau_\theta) = I_0 \exp(-\tau_\theta/\sigma) \quad (\tau_{\theta,\min} \leq \tau_\theta). \quad (83)$$

Here we take $\tau_{\theta,\min} = 0$ to make Figs. 21 and 22. Other parameters are the same as those adopted in Figs. 17 and 18.

We can conclude from these figures that sudden deeming local pulses (either short or long) would give rise to sharp features of the light curves (see Figs. 13, 14, 19 and 20); short linear decay local pulses would also lead to light curves with sharp features (see Figs. 11 and 15); exponential decay local pulses (either short or long) would give rise to smooth light curves (see Figs. 17, 18, 21 and 22); long gradually deeming local pulses would give birth to smooth light curves (see Figs. 12, 16, 18 and 22).

We notice that, even though sudden deeming local pulses would give rise to sharp features of the light curves, suddenly shining local pulses would not. This must be due to the fact that the former would give up their roles to the Doppler effect of the surface after the deeming begins, while the latter would not.

5 Discussion and conclusions

In this paper, we study light curves of pulses of gamma-ray bursts affected by the Doppler effect of the expanding fireball surface, where we pay most of our attention to the effect arising from the the limit of the time delay due to the curvature of the surface. In section 2, we present formula of the count rate in terms of the integral of time derived in detailed for highly symmetric fireballs. In section 3, we apply a local δ function form of pulses to the formula and obtain the light curve of pulses of fireballs ignoring the effect of the local pulse width, where previous results are compared. In section 4, we study the light curve of local pulses lasting an interval of time, including local rectangle pulses as well as other forms of pulses.

One of the interesting results is that the previous suggestion that the well known structure of FRED of pulses could be accounted for by the curvature effect of bursts (here, the Doppler effect of expanding fireballs), where the exponential decay phase is due to the curvature effect while the rising portion is produced by the width of the local pulse (the smaller the width of the local pulse, the narrower the observed rising phase), is convinced by our much detailed analysis which does

not rely on any approximately valued quantities or estimated methods. The conclusion is thus quite robust in the theoretical ground. We find that this character of FRED is independent of the Lorentz factor as long as the factor is large enough to represent a relativistic motion, and it is independent of the local structure of pulses. This indicates that the FRED structure is indeed a consequence of the expanding motion of fireballs. The size of the fireball provides a limit to the observation time, but it is interesting that this limit does not prevent the formation of the exponential decay tail.

Shown by the analysis, both the observed peak and width of the count rate of a very narrow local pulse are proportional to the size of the fireball. The former rises linearly with respect to the increase of the Lorentz factor. As was previously pointed out (see, e.g. Fenimore et al. 1993), the latter decays rapidly following the law of Γ^{-2} , which could account for the phenomenon shown in many bursts that very short time scales, as small as a few *ms*, of pulses are observed. (If the range of the Lorentz factor is $\Gamma \sim 10 - 100$, then the observed width of the light curve of a very narrow local pulse would be $\sim 0.002 - 0.00002$ times smaller than the time scale of the real size of the fireball. It is known that, a size of 1500km corresponds to a time scale of 5ms . When $\Gamma = 10$, the observed 5ms time scale would correspond to a size of $7.5 \times 10^5\text{km}$; while when $\Gamma = 100$ it would correspond to that of $7.5 \times 10^7\text{km}$.) For a certain value of the Lorentz factor, the peak and the width are proportional to each other. We find that, for a same kind of fireball sources, if their difference is merely due to the Lorentz factor, the product of the square of the peak count rate and the width of the light curve of their very narrow local pulses would be the same, which provides a statistical approach to test the fireball model with pulses of GRBs. For a source, if the intensity of its pulses remains unchanged, one can expect a high pulse coupling with a small width and a low pulse coupling with a large one.

It is pointed out that, due to the Doppler effect of the fireball surface, neglecting the area of $\theta > 1/\Gamma$ would lead a light curve, of a very narrow local pulse, with a cutoff tail in its decay phase, which we call a cutoff tail problem. If the local pulse concerned is short enough, this feature would become a criterion to pick out those sources with $\theta < 1/\Gamma$ from others. Note that, as the count rate at $\theta = 1/\Gamma$ is a quarter of the peak, the feature would be obviously observable.

To find the impact of the rest frame radiation on the light curve, we adopt a typical Band function form of radiation to make the light curve and find that the impact can be very obvious.

The analysis reveals that sudden deeming local pulses (either short or long) or short linear decay local pulses would give rise to sharp features of light curves, while exponential decay local pulses (either short or long) or long gradually deeming local pulses would lead to smooth light curves. With the observed feature of light curves, one can figure out the structure of the original pulses.

The interval ($\Delta\tau_{pb}$) between the observed beginning and the peak of the light curve of a local rectangle pulse is proportional to the local width of the pulse (see Appendix B for a detailed analysis). For a large value of the Lorentz factor, the peak count rate (C_p) of the light curve of local rectangle pulses would be proportional to $1/\Gamma^4\beta^2(1-\beta)^3$. With the two quantities we get

$$\frac{C_p}{\Delta\tau_{pb}} \propto \frac{\Gamma^4}{\Delta\tau_\theta} \quad (\Gamma \gg 1). \quad (84)$$

It indicates that the slope of the up rising part of an FRED pulse, if it arises from a local pulse with a constant emission, would be very sensitive to the Lorentz factor and be sensitive to the rest fame width of the pulse as well. Therefore, quantity $C_p/\Delta\tau_{pb}$ of pulses might be useful for detecting the expanding speed of some GRBs.

As is shown above, our analysis bases on the model of fireballs which are highly symmetric and expand relativistically. However, since the derivation does not rely on any estimated methods, the basic formulas (those in section 2) are applicable to sub-relativistic cases as well as non-relativistic cases as long as the objects concerned are highly symmetric and isotropically expand. In our derivation, the thickness of the outer shell is not taken into account. This does not matter. In the analysis, the concept of the surface intensity is employed. Any radiation from the shell must pass through the surface and at any time there is a unique value of radiation passing through it, and this is the quantity defined as the surface density. In this way, all radiations from the shell or even behind the shell are included.

It is interesting that, even though our analysis bases on the model of highly symmetric fireballs, the formula is applicable to small area such as $\theta \leq 1/\Gamma$ as long as the area concerned is locally highly symmetric. If all GRBs are beamed, the discussion of the case of the whole fireball surface would become meaningless. However, since light curves of the GRBs observed vary enormously, we suspect that there might be various models accounting for all of these objects. Due to the great output rate of the radiation observed, many GRBs would undergo the fireball state and some of them might probably be observed when they remain in the fireball stage. These sources would be

best accounted for by the fireball model.

Appendix A. Relation between the peak count rate and the width of $C_0(\tau)$

Here, we employ the concept of FWHM to describe the width of $C_0(\tau)$.

One can verify from (36) that the maximum value of $C_0(\tau)$ would be obtained when $\tau \rightarrow (1 - \beta)\tau_{\theta,0}$. Let

$$C_{0,p} \equiv C_0[\tau \rightarrow (1 - \beta)\tau_{\theta,0}]. \quad (A1.)$$

Then, from (36) we obtain

$$C_{0,p} = \frac{1 + \beta\tau_{\theta,0}}{\Gamma^3(1 - \beta)^2}. \quad (A2.)$$

Applying (A2.), when $\beta > 0$, one can obtain from (36) that

$$\tau_H = \frac{-(1 + k + \beta\tau_{\theta,0}) + (1 + \beta\tau_{\theta,0})\sqrt{k^2 + (1 + k)^2}}{k^2}, \quad (A3.)$$

where

$$C_0(\tau = \tau_H) = \frac{C_{0,p}}{2}. \quad (A4.)$$

Therefore, the width, described by the concept of FWHM, of the light curve of the local δ function pulse would be

$$\Delta\tau_{FWHM} = \tau_H - (1 - \beta)\tau_{\theta,0} = \frac{(\Gamma - \sqrt{\Gamma^2 - 1})(\sqrt{2\Gamma^2 - 1} - \Gamma)}{\Gamma^2 - 1}(1 + \beta\tau_{\theta,0}). \quad (A5.)$$

From (39) we learn that the interval of the observable time of the local δ function pulse is

$$\Delta\tau = 1 + \tau_{\theta,0} - (1 - \beta)\tau_{\theta,0} = 1 + \beta\tau_{\theta,0}. \quad (A6.)$$

According to Paper III, the radius of the fireball at time t_θ can be determined by

$$R(t_\theta) = (t_\theta - t_c)\beta c + R_c. \quad (A7.)$$

Inserting (32) to (A7.) we find

$$1 + \beta\tau_{\theta,0} = \frac{R(t_{\theta,0})}{R_c}. \quad (A8.)$$

Thus, $\Delta\tau$ represents, in a relative term, the time scale of the real size of the fireball at the corresponding emission time, $t_{\theta,0}$. Applying (A8.) we get from (A5.) that

$$\Delta\tau_{FWHM} = \frac{(\Gamma - \sqrt{\Gamma^2 - 1})(\sqrt{2\Gamma^2 - 1} - \Gamma)}{\Gamma^2 - 1} \frac{R(t_{\theta,0})}{R_c}. \quad (A9.)$$

From (A2.) one finds

$$C_{0,p} = \frac{1}{\Gamma(\Gamma - \sqrt{\Gamma^2 - 1})^2} \frac{R(t_{\theta,0})}{R_c}, \quad (A10.)$$

where, (A8.) is applied. Combining (A9.) and (A10.) we get

$$C_{0,p} = \frac{\Gamma^2 - 1}{\Gamma(\Gamma - \sqrt{\Gamma^2 - 1})^3 (\sqrt{2\Gamma^2 - 1} - \Gamma)} \Delta\tau_{FWHM}. \quad (A11.)$$

This is the relation between the peak count rate and the width of $C_0(\tau)$.

Inserting (A2.) into (36) yields

$$\frac{C_0(\tau)}{C_{0,p}} = \frac{\left(\frac{\Delta\tau}{\beta} - \frac{1}{k} - \tau\right)\Delta\tau}{(1 + k\tau)^2}, \quad (A12.)$$

where (A6.) is applied. With this, the ratio of a certain count rate to the peak count rate of $C_0(\tau)$ with respect to the observation time is determined. An important application of this is to consider the case of $\theta_{\max} = 1/\Gamma$, for which we obtain the maximum value of τ from (51). Applying this value to (A12.) and assuming $\Gamma \gg 1$ we get

$$C_0(\tau|_{\theta=1/\Gamma}) \simeq \frac{C_{0,p}}{4}. \quad (A13.)$$

Appendix B. Peak count rate of the light curve of local rectangle pulses ignoring the rest frame spectral form

Here we present a detailed study on the peak count rate of the light curve of a local rectangle pulse with its rest frame spectrum being a δ function form, for which the count rate is determined by (71).

We consider the case of the whole fireball surface for which (38) is applied. In this case (72), (73) and (74) are applicable. From (74) we find that, if

$$(1 - \beta)\tau_{\theta,\max} < 1 + \tau_{\theta,\min}, \quad (B1.)$$

there will be three ranges of τ : $I_I \equiv \{(1 - \beta)\tau_{\theta,\min} \leq \tau \leq (1 - \beta)\tau_{\theta,\max}\}$, $I_{II} \equiv \{(1 - \beta)\tau_{\theta,\max} \leq \tau \leq 1 + \tau_{\theta,\min}\}$, and $I_{III} \equiv \{1 + \tau_{\theta,\min} \leq \tau \leq 1 + \tau_{\theta,\max}\}$. If

$$1 + \tau_{\theta,\min} < (1 - \beta)\tau_{\theta,\max}, \quad (B2.)$$

there will be three other ranges of τ : $II_I \equiv \{(1 - \beta)\tau_{\theta,\min} \leq \tau \leq 1 + \tau_{\theta,\min}\}$, $II_{II} \equiv \{1 + \tau_{\theta,\min} \leq \tau \leq (1 - \beta)\tau_{\theta,\max}\}$, and $II_{III} \equiv \{(1 - \beta)\tau_{\theta,\max} \leq \tau \leq 1 + \tau_{\theta,\max}\}$.

One can check that, in range I_I , $\tilde{\tau}_{\theta,\min} = \tau_{\theta,\min}$ and $\tilde{\tau}_{\theta,\max} = \tau/(1-\beta)$, and then we get from (71) that

$$\frac{C(\tau)}{\frac{2\pi R_c^3 I_0}{5\nu_0 hc D^2 \Gamma^4 \beta^2 (1-\beta)^3} \left\{ \frac{(5\beta-1)(1+k\tau)^2}{4} + \frac{5(1-\beta)(1+\beta\tau_{\theta,\min})^4}{4(1+k\tau)^2} - \frac{(1+\beta\tau_{\theta,\min})^5}{(1+k\tau)^3} \right\}}, \quad (B3.)$$

in range I_{II} , $\tilde{\tau}_{\theta,\min} = \tau_{\theta,\min}$ and $\tilde{\tau}_{\theta,\max} = \tau_{\theta,\max}$, and then we get

$$\frac{C(\tau)}{\frac{2\pi R_c^3 I_0}{5\nu_0 hc D^2 \Gamma^4 \beta^2 (1-\beta)^3} \left\{ \frac{(1+\beta\tau_{\theta,\max})^5 - (1+\beta\tau_{\theta,\min})^5}{(1+k\tau)^3} - \frac{5[(1+\beta\tau_{\theta,\max})^4 - (1+\beta\tau_{\theta,\min})^4]}{4(1-\beta)^{-1}(1+k\tau)^2} \right\}}, \quad (B4.)$$

in range I_{III} , $\tilde{\tau}_{\theta,\min} = \tau - 1$ and $\tilde{\tau}_{\theta,\max} = \tau_{\theta,\max}$, and then we get

$$\frac{C(\tau)}{\frac{2\pi R_c^3 I_0}{5\nu_0 hc D^2 \Gamma^4 \beta^2 (1-\beta)^3} \left\{ \frac{(1+\beta\tau_{\theta,\max})^5}{(1+k\tau)^3} - \frac{5(1-\beta)(1+\beta\tau_{\theta,\max})^4}{4(1+k\tau)^2} + \frac{(1-\beta)^5(1+k\tau)^2}{4} \right\}}, \quad (B5.)$$

in range $II_I \equiv$, $\tilde{\tau}_{\theta,\min} = \tau_{\theta,\min}$ and $\tilde{\tau}_{\theta,\max} = \tau/(1-\beta)$, then we get (B3.); in range II_{II} , $\tilde{\tau}_{\theta,\min} = \tau - 1$ and $\tilde{\tau}_{\theta,\max} = \tau/(1-\beta)$, and then we get

$$C(\tau) = \frac{2\pi R_c^3 I_0}{5\nu_0 hc D^2 \Gamma^4 \beta^2 (1-\beta)^3} \frac{5\beta - 1 + (1-\beta)^5}{4} (1+k\tau)^2; \quad (B6.)$$

in range II_{III} , $\tilde{\tau}_{\theta,\min} = \tau - 1$ and $\tilde{\tau}_{\theta,\max} = \tau_{\theta,\max}$, and then we get (B5.).

In this paper, we pay our attention mainly to relativistic motions, and hence we assume

$$\beta > \frac{3}{5} \quad (B7.)$$

in the following analysis.

a) In the case of $(1-\beta)\tau_{\theta,\max} < 1 + \tau_{\theta,\min}$, we have (B3.) in range I_I , (B4.) in range I_{II} and (B5.) in range I_{III} . Differentiating (B3.), (B4.), and (B5.) we obtain

$$= \frac{\pi R_c^3 I_0}{5\nu_0 hc D^2 \Gamma^4 \beta (1-\beta)^4} \frac{\frac{dC(\tau)}{d\tau}}{\frac{[(5\beta-1)(1+k\tau)^4 - 5(1-\beta)(1+\beta\tau_{\theta,\min})^4](1+k\tau) + 6(1+\beta\tau_{\theta,\min})^5}{(1+k\tau)^4}}, \quad (B8.)$$

$$= \frac{\pi R_c^3 I_0}{5\nu_0 hc D^2 \Gamma^4 \beta (1-\beta)^4} \frac{\frac{d}{d\tau} C(\tau)}{\frac{5[(1+\beta\tau_{\theta,\max})^4 - (1+\beta\tau_{\theta,\min})^4](1+k\tau) - 6[(1+\beta\tau_{\theta,\max})^5 - (1+\beta\tau_{\theta,\min})^5]}{(1+k\tau)^4}}, \quad (B9.)$$

and

$$= \frac{\pi R_c^3 I_0}{5\nu_0 hc D^2 \Gamma^4 \beta (1-\beta)^4} \frac{\frac{d}{d\tau} C(\tau)}{\frac{[(1-\beta)^4(1+k\tau)^4 + 5(1+\beta\tau_{\theta,\max})^4](1-\beta)(1+k\tau) - 6(1+\beta\tau_{\theta,\max})^5}{(1+k\tau)^4}}, \quad (B10.)$$

respectively.

One finds $\beta\tau_{\theta,\min} \leq k\tau \leq \beta\tau_{\theta,\max}$ in range I_I , $(1-\beta)(1+k\tau) \leq 1 + \beta\tau_{\theta,\min}$ in range I_{II} , and $(1-\beta)(1+k\tau) \leq (1 + \beta\tau_{\theta,\max})$ in range I_{III} . Therefore,

$$\begin{aligned} & (5\beta-1)(1+k\tau)^4 - 5(1-\beta)(1+\beta\tau_{\theta,\min})^4 \\ & \geq 2(5\beta-3)(1+\beta\tau_{\theta,\min})^4 > 0 \quad (\tau \in I_I), \end{aligned} \quad (B11.)$$

$$\begin{aligned} & 5[(1 + \beta\tau_{\theta,\max})^4 - (1 + \beta\tau_{\theta,\min})^4](1 - \beta)(1 + k\tau) - 6[(1 + \beta\tau_{\theta,\max})^5 - (1 + \beta\tau_{\theta,\min})^5] \\ & \leq -[(1 + \beta\tau_{\theta,\max})^4 - (1 + \beta\tau_{\theta,\min})^4](1 + \beta\tau_{\theta,\min}) \leq 0 \quad (\tau \in I_{III}), \end{aligned} \quad (B12.)$$

$$[(1 - \beta)^4(1 + k\tau)^4 + 5(1 + \beta\tau_{\theta,\max})^4](1 - \beta)(1 + k\tau) - 6(1 + \beta\tau_{\theta,\max})^5 \leq 0 \quad (\tau \in I_{III}). \quad (B13.)$$

In this case, $dC(\tau)/d\tau > 0$ in range I_I , $dC(\tau)/d\tau \leq 0$ in range I_{II} , and $dC(\tau)/d\tau \leq 0$ in range I_{III} . Hence, the peak of $C(\tau)$ must be located at the upper limit of τ in range I_I . That is

$$C_{I,p} = C[\tau = (1 - \beta)\tau_{\theta,\max}] \\ = \frac{2\pi R_c^3 I_0}{5\nu_0 hc D^2 \Gamma^4 \beta^2 (1 - \beta)^3} \left\{ \frac{(1 + \beta\tau_{\theta,\max})^5 - (1 + \beta\tau_{\theta,\min})^5}{(1 + \beta\tau_{\theta,\max})^3} - \frac{5(1 - \beta)[(1 + \beta\tau_{\theta,\max})^4 - (1 + \beta\tau_{\theta,\min})^4]}{4(1 + \beta\tau_{\theta,\max})^2} \right\}. \quad (B14.)$$

b) In the case of $1 + \tau_{\theta,\min} < (1 - \beta)\tau_{\theta,\max}$, we have (B3.) in range II_I , (B6.) in range II_{III} and (B5.) in range II_{III} . Differentiating (B3.) and (B5.) we obtain (B8.) and (B10.), respectively. Differentiating (B6.) we get

$$\frac{d}{d\tau} C(\tau) = \frac{\pi R_c^3 I_0}{5\nu_0 hc D^2 \Gamma^4 \beta (1 - \beta)^4} [(1 - \beta)^5 + 5\beta - 1](1 + k\tau). \quad (B15.)$$

We find $\beta\tau_{\theta,\min} \leq k\tau$ in range II_I and $(1 - \beta)(1 + k\tau) \leq (1 + \beta\tau_{\theta,\max})$ in range II_{III} . In the same way, one reaches $dC(\tau)/d\tau > 0$ in range II_I and $dC(\tau)/d\tau \leq 0$ in range II_{III} . Since $\beta > \frac{3}{5}$, we find that

$$(1 - \beta)^5 + 5\beta - 1 > (1 - \beta)^5 + 2 > 0. \quad (B16.)$$

Hence, $dC(\tau)/d\tau > 0$ in range II_{III} . Therefore, the peak of $C(\tau)$ must be located at the upper limit of τ in range II_{III} . That is

$$C_{II,p} = C[\tau = (1 - \beta)\tau_{\theta,\max}] \\ = \frac{2\pi R_c^3 I_0}{5\nu_0 hc D^2 \Gamma^4 \beta^2 (1 - \beta)^3} \frac{[(1 - \beta)^5 + 5\beta - 1](1 + \beta\tau_{\theta,\max})^2}{4}. \quad (B17.)$$

As shown above, when $\beta > \frac{3}{5}$, the position of the peak count rate of the light curve of local rectangle pulses would be located at $\tau = (1 - \beta)\tau_{\theta,\max}$. Therefore, according to (74), the interval between the beginning and the peak of the pulse would be

$$\Delta\tau_{pb} \equiv (1 - \beta)\tau_{\theta,\max} - (1 - \beta)\tau_{\theta,\min} = (1 - \beta)(\tau_{\theta,\max} - \tau_{\theta,\min}). \quad (B18.)$$

Let

$$\Delta\tau_\theta \equiv \tau_{\theta,\max} - \tau_{\theta,\min}. \quad (B19.)$$

One finds

$$\Delta\tau_{pb} = (1 - \beta)\Delta\tau_\theta. \quad (B20.)$$

It suggests that the interval between the observed beginning and the peak of the light curve of a local rectangle pulse is proportional to the local width of the pulse. For a same kind of local rectangle pulses, $\Delta\tau_{pb}$ would become an indicator of the Lorentz factor of the expanding fireball.

From (B20.) one finds that, when $\Delta\tau_\theta \rightarrow 0$, $\Delta\tau_{pb} \rightarrow 0$. The profile would approach that of local δ function pulses.

From (B14.) and (B17.) we find that, when $\Gamma \gg 1$, the peak of the count rate would be proportional to $1/\Gamma^4\beta^2(1-\beta)^3$. Let C_p be the observed peak count rate of a pulse. One can check that

$$\frac{C_p}{\Delta\tau_{pb}} \propto \frac{\Gamma^4}{\Delta\tau_\theta} \quad (\Gamma \gg 1). \quad (B21.)$$

This indicates that the slope of the up rising part of an FRED pulse, if it can be described by the light curve of a local rectangle pulse, would be very sensitive to the Lorentz factor and be sensitive to the width of the local pulse as well.

Quantities $\Delta\tau_{pb}$ and $C_p/\Delta\tau_{pb}$ of pulses might be useful for detecting the expanding speed of GRBs, so long as the pulses can be described by the light curve of local rectangle pulses.

References

Band, D., et al. 1993, *ApJ*, 413, 281

Goodman, J. 1986, *ApJ*, 308, L47

Fenimore, E. E., Epstein, R. I., and Ho, C. 1993, *A&AS*, 97, 59

Fenimore, E. E., Madras, C. D., and Nayakshin, S. 1996, *ApJ*, 473, 998 (Paper I)

Fishman, G. J., et al. 1994, *ApJS*, 92, 229

Ford, L. A., Band, D. L., Matteson, J. L., et al. 1995, *ApJ*, 439, 307

Hailey, C. J., Harrison, F. A., and Mori, K. 1999, *ApJ*, 520, L25

Kocevski, D., Ryde, F., and Liang, E. 2003, *ApJ*, 596, 389

Krolik, J. H., & Pier, E. A. 1991, *ApJ*, 373, 277

Norris, J. P., Nemiroff, R. J., and Bonnell, J. T. et al. 1996, *ApJ*, 459, 393

Mészáros, P., and Rees, M. J. 1998, *ApJ*, 502, L105

Paczynski, B. 1986, *ApJ*, 308, L43

Preece, R. D., Pendleton, G. N., Briggs, M. S., et al. 1998, *ApJ*, 496, 849

Preece, R. D., Briggs, M. S., Mallozzi, R. S., et al. 2000, *ApJS*, 126, 19

Qin, Y.-P. 2002, *A&A*, 396, 705 (Paper III)

Qin, Y.-P. 2003, *A&A*, 407, 393

Ryde, F., and Petrosian, V. 2002, *ApJ*, 578, 290 (Paper II)

Schaefer, B. E., Teegaeden, B. J., Fantasia, S. F., et al. 1994, *ApJS*, 92, 285

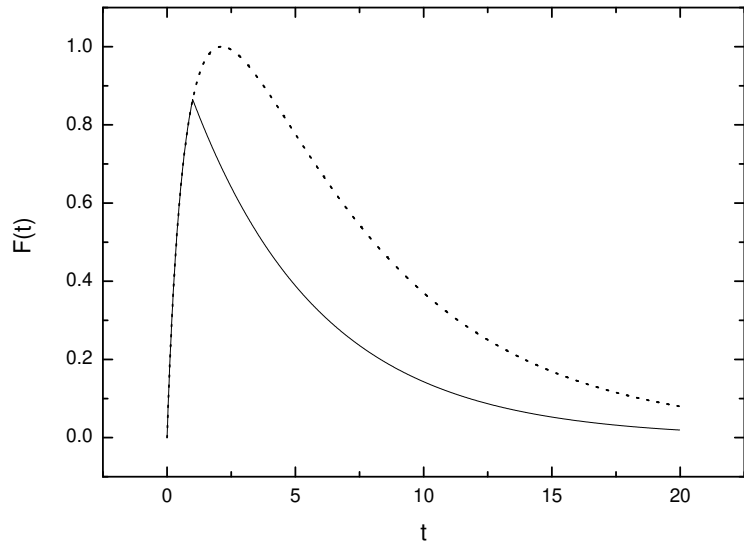


Figure 1: The plot of $F(t) — t$ for the light curve of equation (1) with $f(t) \propto \exp(-t/t_{dyn})$, $(0 < t < \infty)$, where we take $t_{dyn} = 5s$ and $t_{ang} = 1s$. The solid line represents the curve integrated from 0 to t_{ang} while the dot line stands for the curve integrated from 0 to ∞ .

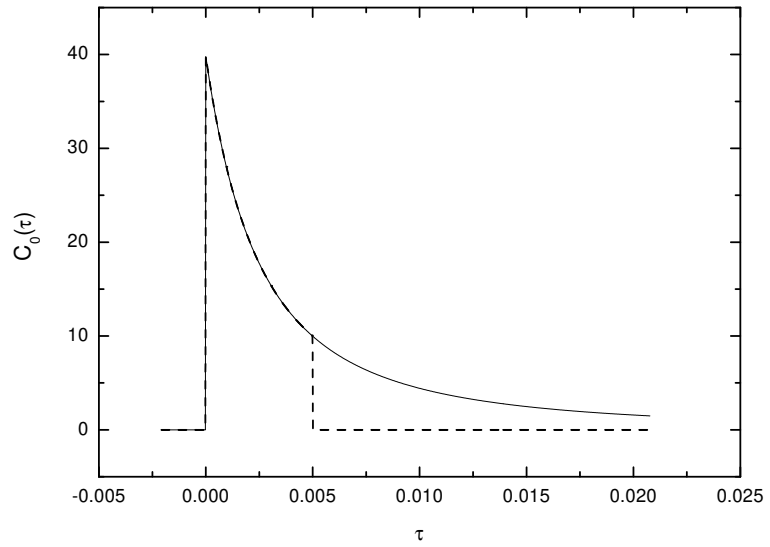


Figure 2: The plot of $C_0(\tau) — \tau$ for the light curve of the local δ function pulse determined by (36), where $\tau_{\theta,0} = 0$ and $\Gamma = 10$. The solid line represents the curve confined by (39) while the dash line stands for the curve confined by (50).

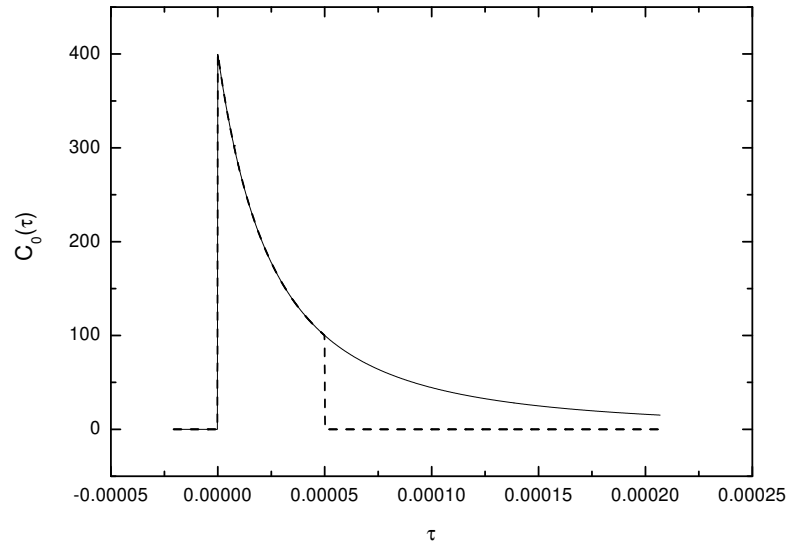


Figure 3: The plot of $C_0(\tau)$ — τ for the light curve of the local δ function pulse determined by (36), where $\tau_{\theta,0} = 0$ and $\Gamma = 100$. The symbols are the same as those adopted in Fig. 2.

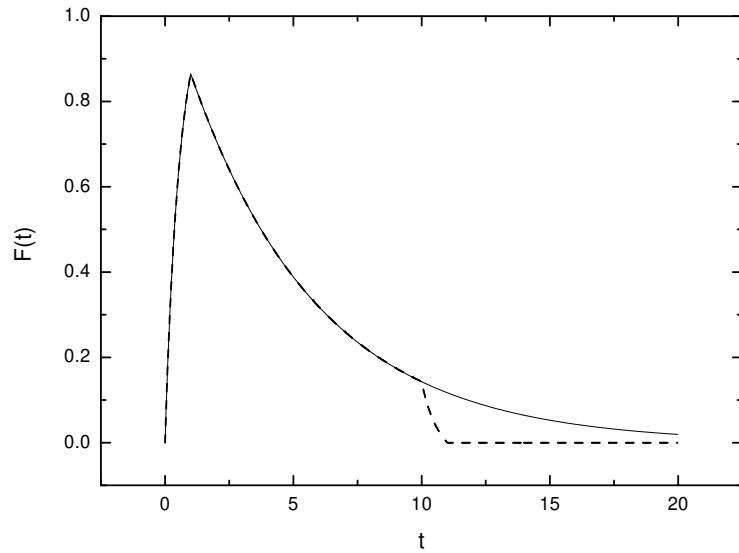


Figure 4: The plot of $F(t)$ — t for the light curve of equation (1) with $f(t) \propto \exp(-t/t_{dyn})$, $(0 < t < t_{dyn})$, where we take $t_{dyn} = 5s$ and $t_{ang} = 1s$. The dash line represents the curve integrated from 0 to t_{ang} , while the solid line is just the solid line in Fig. 1.

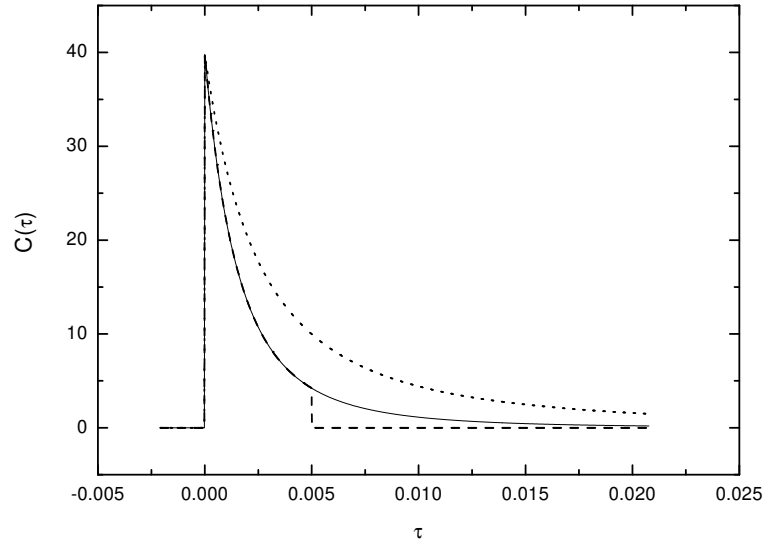


Figure 5: The plot of $C(\tau)$ — τ for the light curve of the local δ function pulse determined by (35), where a Band function rest frame radiation form is adopted, and we take $\tau_{\theta,0} = 0$ and $\Gamma = 10$. The dot line is the solid line in Fig. 2. The solid line represents the curve confined by (39), which is normalized to the peak of the dot line, and the dash line stands for the curve confined by (50), which shares the same magnitude constant of the solid line.

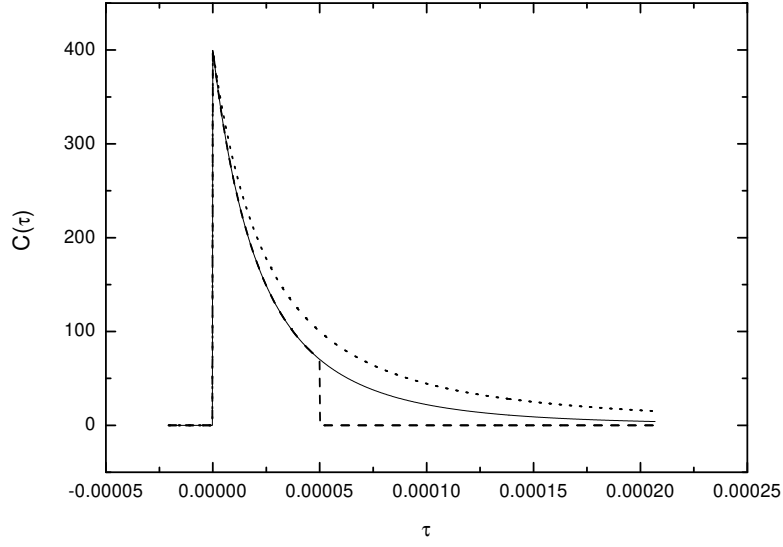


Figure 6: The plot of $C(\tau)$ — τ for the light curve of the local δ function pulse determined by (35), where a Band function rest frame radiation form is adopted, and we take $\tau_{\theta,0} = 0$ and $\Gamma = 100$. The dot line is the solid line in Fig. 3. The solid line represents the curve confined by (39), which is normalized to the peak of the dot line, and the dash line stands for the curve confined by (50), which shares the same magnitude constant of the solid line.

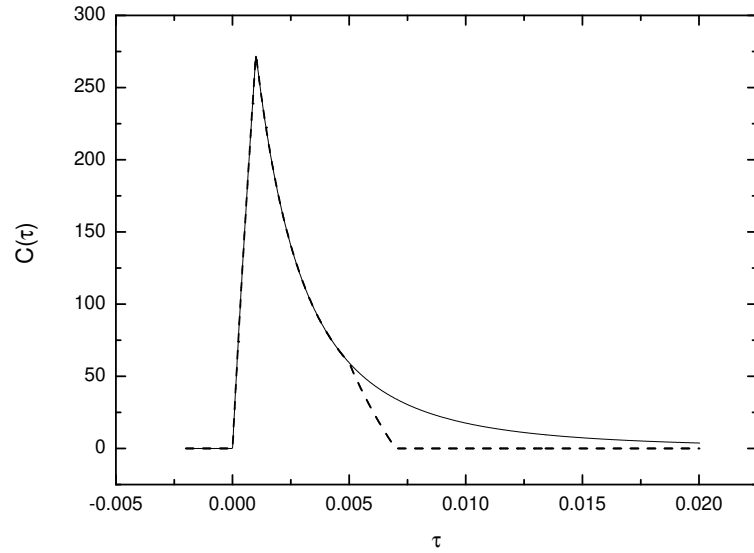


Figure 7: The plot of $C(\tau) — \tau$ for the light curve of the local rectangle pulse determined by (71), where we take $\Gamma = 10$, $\tau_{\theta,min} = 0$ and $\tau_{\theta,max} = 0.2$. The solid line represents the curve corresponding to the whole fireball surface while the dash line stands for the curve associated with the small area of the surface of $\theta \leq 1/\Gamma$.

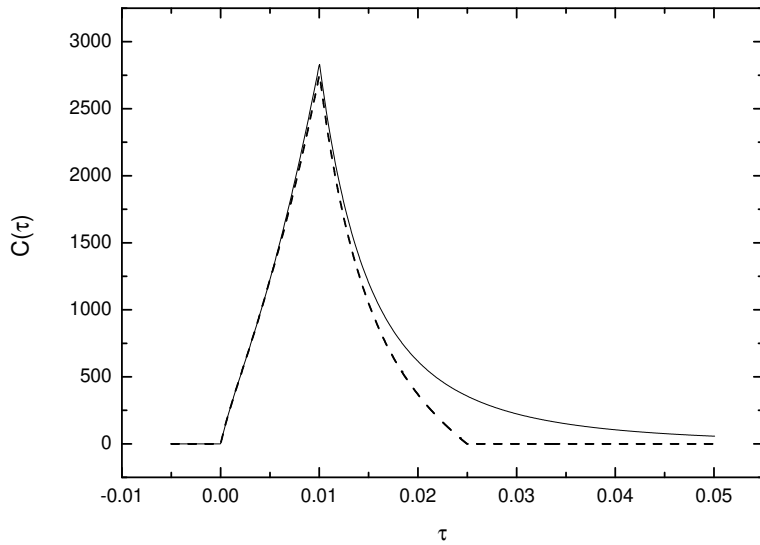


Figure 8: The plot of $C(\tau) — \tau$ for the light curve of the local rectangle pulse determined by (71), where we take $\Gamma = 10$, $\tau_{\theta,min} = 0$ and $\tau_{\theta,max} = 2$. The symbols are the same as those adopted in Fig. 7.

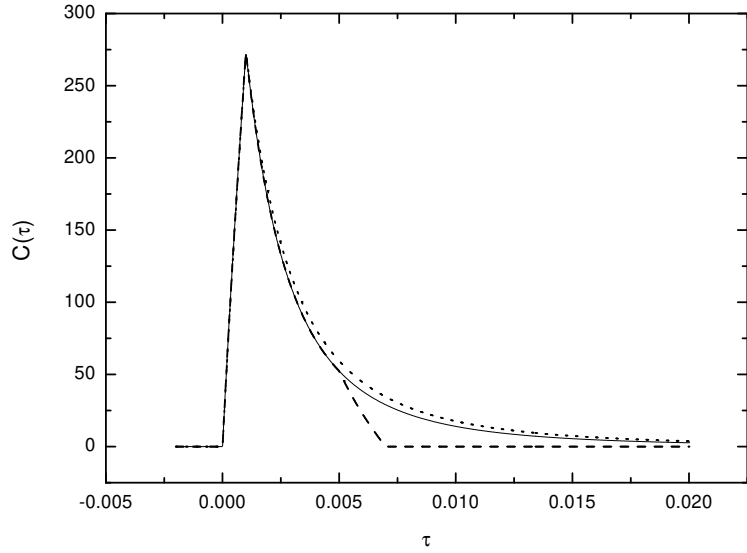


Figure 9: The plot of $C(\tau) — \tau$ for the light curve of the local rectangle pulse determined by (57), where a Band function rest frame radiation form is adopted, and we take $\Gamma = 10$, $\tau_{\theta,min} = 0$ and $\tau_{\theta,max} = 0.2$. The dot line is the solid line in Fig. 7. The solid line represents the curve corresponding to the whole fireball surface, which is normalized to the peak of the dot line, while the dash line stands for the curve associated with the small area of the surface of $\theta \leq 1/\Gamma$, which shares the same magnitude constant of the solid line.

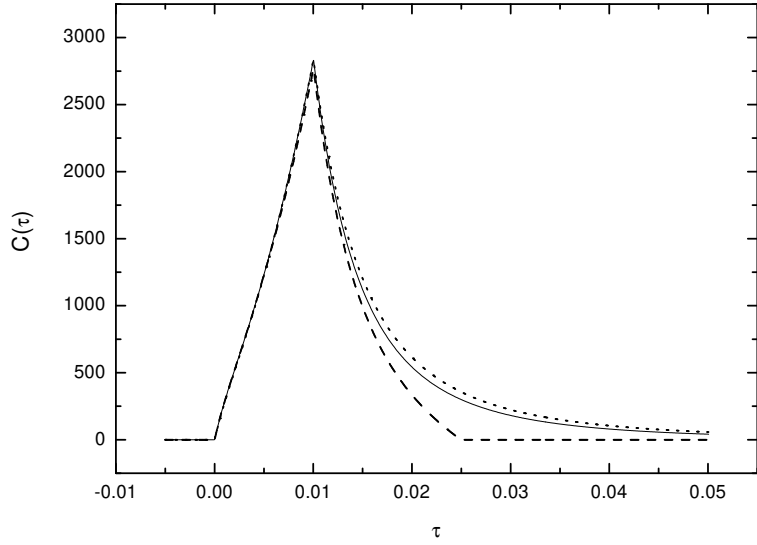


Figure 10: The plot of $C(\tau) — \tau$ for the light curve of the local rectangle pulse determined by (57), where a Band function rest frame radiation form is adopted, and we take $\Gamma = 10$, $\tau_{\theta,min} = 0$ and $\tau_{\theta,max} = 2$. The dot line is the solid line in Fig. 8. Other symbols are the same as those adopted in Fig. 9.

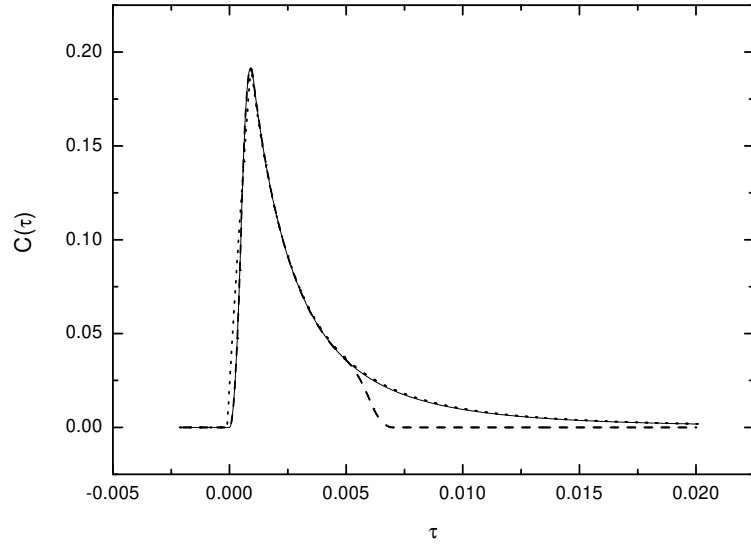


Figure 1: The plot of $C(\tau)$ — τ for the light curve, of the local pulse with the intensity of (78), determined by (21), where a Band function rest frame radiation form is adopted, and we take $\Gamma = 10$, $\tau_{\theta,min} = 0$ and $\tau_{\theta,max} = 0.2$. The dot line is the solid line in Fig. 9, which is normalized to the solid line presented here. The solid line represents the curve corresponding to the whole fireball surface while the dash line stands for the curve associated with the small area of the surface of $\theta \leq 1/\Gamma$.

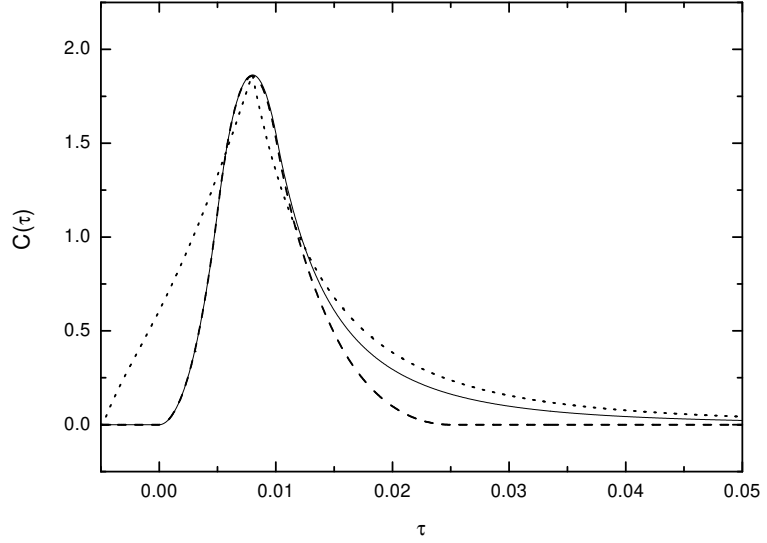


Figure 2: The plot of $C(\tau)$ — τ for the light curve, of the local pulse with the intensity of (78), determined by (21), where a Band function rest frame radiation form is adopted, and we take $\Gamma = 10$, $\tau_{\theta,min} = 0$ and $\tau_{\theta,max} = 2$. The dot line is the solid line in Fig. 10, which is normalized to the solid line presented here. Other symbols are the same as those adopted in Fig. 11.

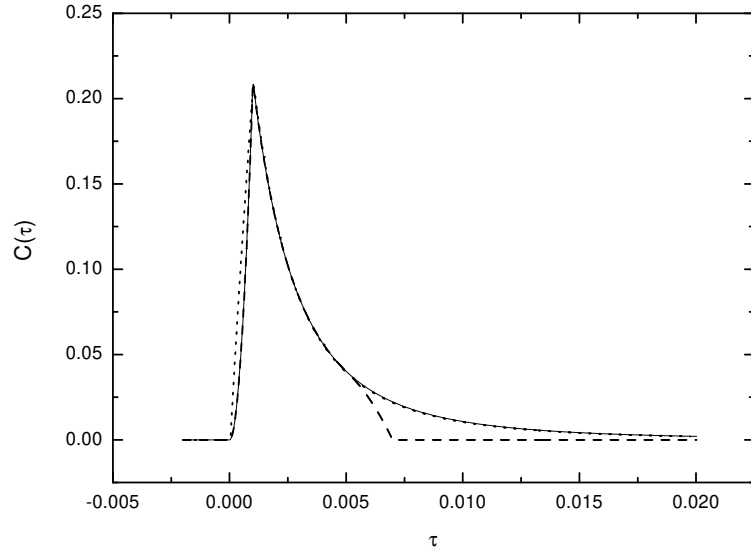


Figure 3: The plot of $C(\tau)$ — τ for the light curve, of the local pulse with the intensity of (79), determined by (21), where a Band function rest frame radiation form is adopted, and we take $\Gamma = 10$, $\tau_{\theta,min} = 0$ and $\tau_{\theta,max} = 0.2$. The symbols are the same as those adopted in Fig. 11.

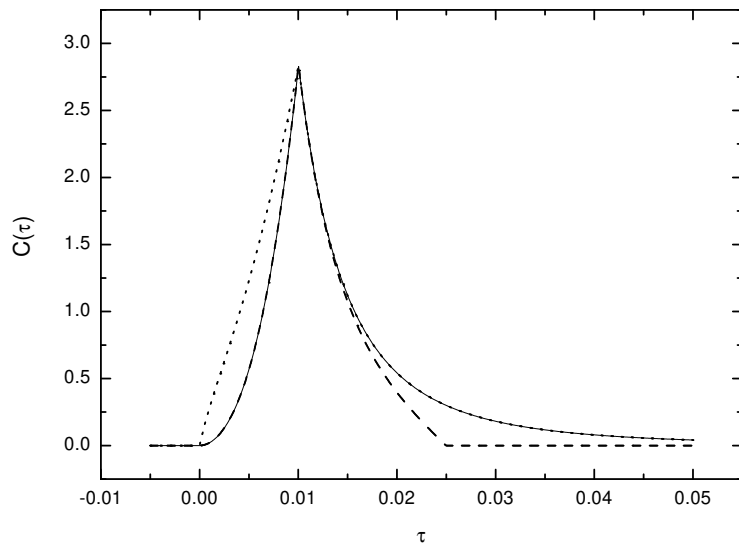


Figure 4: The plot of $C(\tau)$ — τ for the light curve, of the local pulse with the intensity of (79), determined by (21), where a Band function rest frame radiation form is adopted, and we take $\Gamma = 10$, $\tau_{\theta,min} = 0$ and $\tau_{\theta,max} = 2$. The symbols are the same as those adopted in Fig. 12.

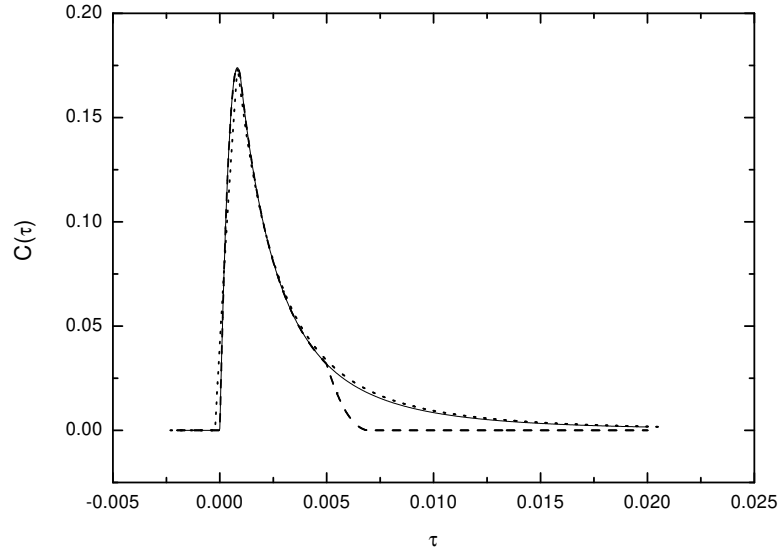


Figure 5: The plot of $C(\tau)$ — τ for the light curve, of the local pulse with the intensity of (80), determined by (21), where a Band function rest frame radiation form is adopted, and we take $\Gamma = 10$, $\tau_{\theta,min} = 0$ and $\tau_{\theta,max} = 0.2$. The symbols are the same as those adopted in Fig. 11.

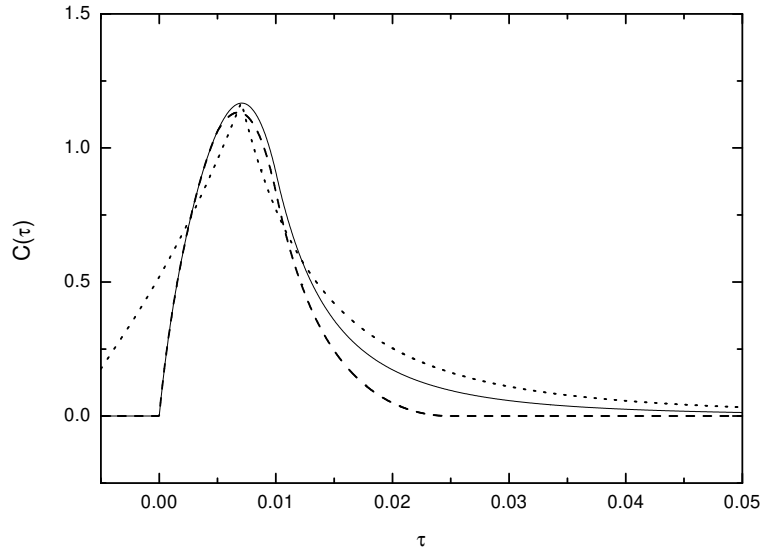


Figure 6: The plot of $C(\tau)$ — τ for the light curve, of the local pulse with the intensity of (80), determined by (21), where a Band function rest frame radiation form is adopted, and we take $\Gamma = 10$, $\tau_{\theta,min} = 0$ and $\tau_{\theta,max} = 2$. The symbols are the same as those adopted in Fig. 12.

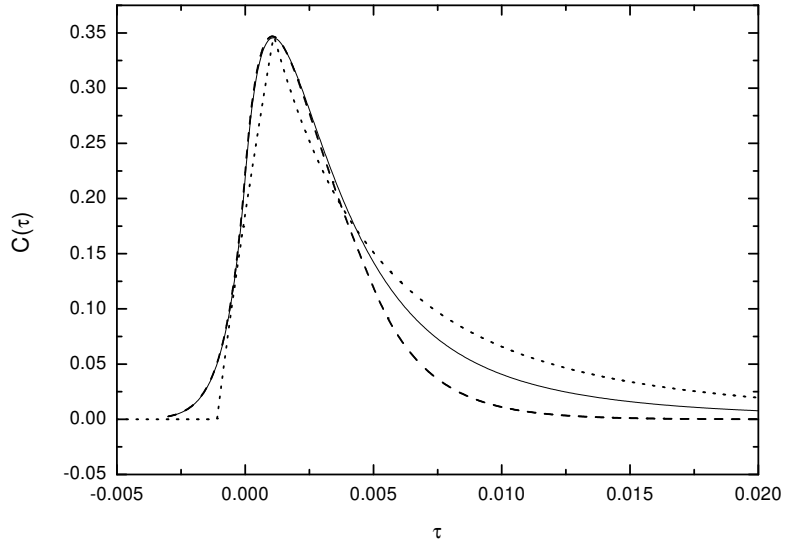


Figure 7: The plot of $C(\tau)$ — τ for the light curve, of the local pulse with the intensity of (81), determined by (21), where a Band function rest frame radiation form is adopted, and we take $\Gamma = 10$, $\tau_{\theta,min} = -1$ and $\sigma = 0.2$. The symbols are the same as those adopted in Fig. 11.

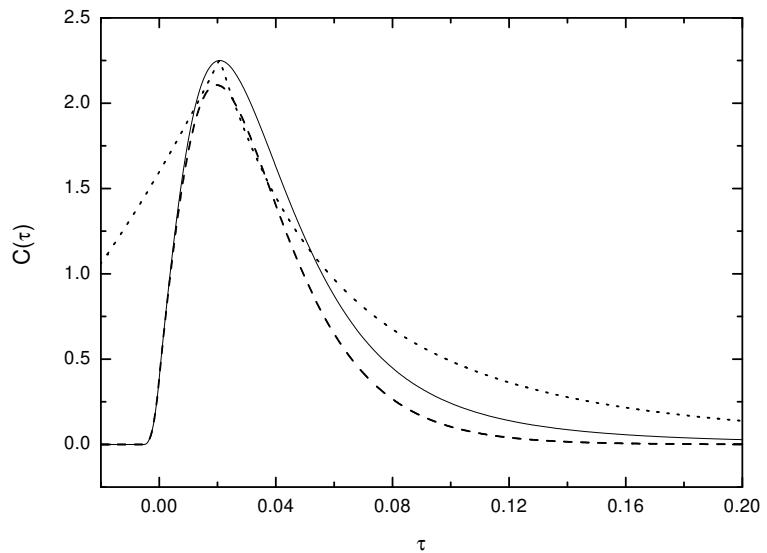


Figure 8: The plot of $C(\tau)$ — τ for the light curve, of the local pulse with the intensity of (81), determined by (21), where a Band function rest frame radiation form is adopted, and we take $\Gamma = 10$, $\tau_{\theta,min} = -1$ and $\sigma = 2$. The symbols are the same as those adopted in Fig. 12.

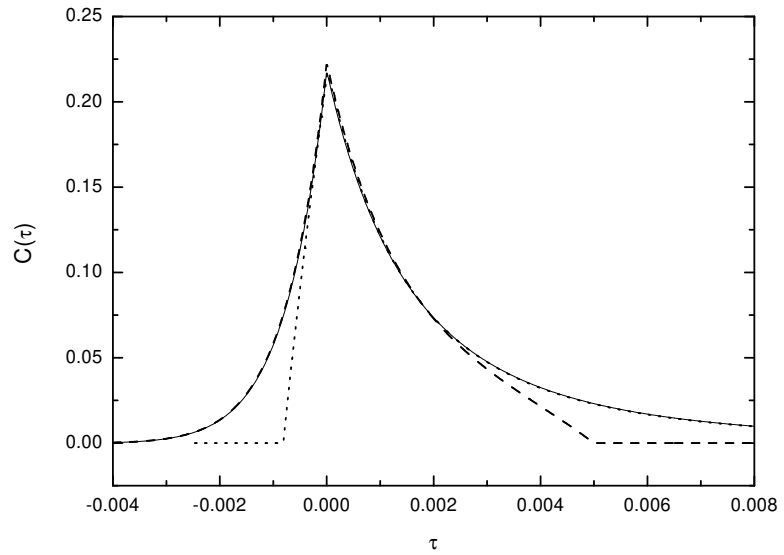


Figure 9: The plot of $C(\tau)$ — τ for the light curve, of the local pulse with the intensity of (82), determined by (21), where a Band function rest frame radiation form is adopted, and we take $\Gamma = 10$, $\tau_{\theta,min} = -1$, $\tau_{\theta,max} = 0$ and $\sigma = 0.2$. The symbols are the same as those adopted in Fig. 11.

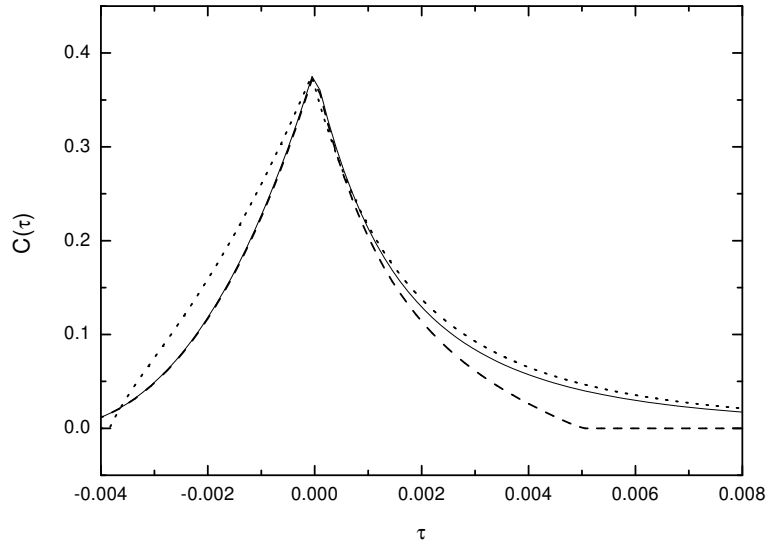


Figure 10: The plot of $C(\tau)$ — τ for the light curve, of the local pulse with the intensity of (82), determined by (21), where a Band function rest frame radiation form is adopted, and we take $\Gamma = 10$, $\tau_{\theta,min} = -1$, $\tau_{\theta,max} = 0$ and $\sigma = 2$. The symbols are the same as those adopted in Fig. 12.

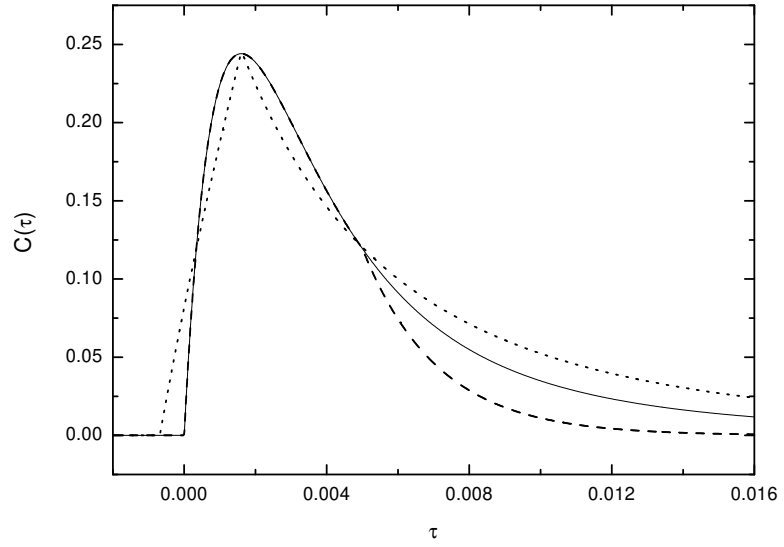


Figure 11: The plot of $C(\tau) — \tau$ for the light curve, of the local pulse with the intensity of (83), determined by (21), where a Band function rest frame radiation form is adopted, and we take $\Gamma = 10$, $\tau_{\theta,min} = 0$ and $\sigma = 0.2$. The symbols are the same as those adopted in Fig. 11.

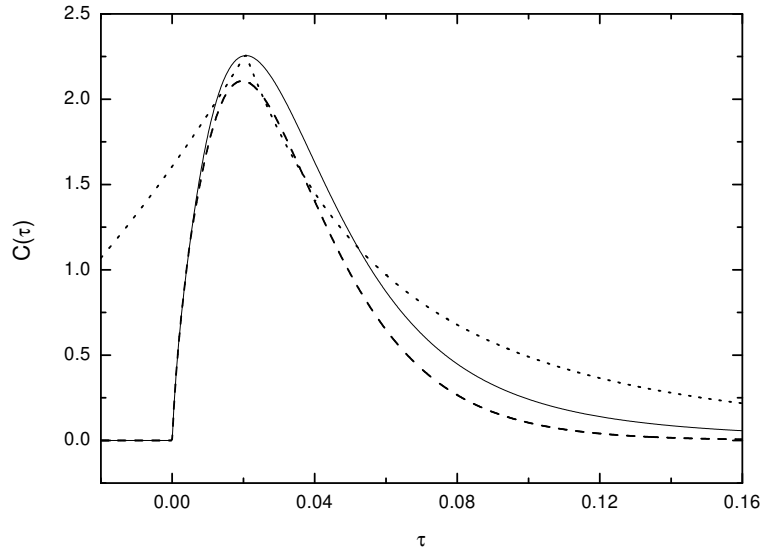


Figure 12: The plot of $C(\tau) — \tau$ for the light curve, of the local pulse with the intensity of (83), determined by (21), where a Band function rest frame radiation form is adopted, and we take $\Gamma = 10$, $\tau_{\theta,min} = 0$ and $\sigma = 2$. The symbols are the same as those adopted in Fig. 12.